

WIRELESS ENGINEER

Vol. XXVII

JULY 1950

No. 322

Surface-Wave Transmission Line

OUR Editorial of June 1936 was entitled "New Type of Wave Transmission"; that was only fourteen years ago, and the new type was the tubular waveguide. In the opening paragraph we referred to the fact, which had been known for many years, that waves can be transmitted along a single wire. We also mentioned that the wire could be either a conductor or a dielectric. The single wire and the tubular waveguide are to some extent complementary, for, starting with a coaxial cable, if the inner conductor is removed, one has a tubular waveguide, whereas, if the outer conductor is removed, one has a single-wire transmission line. In both cases the electric field, instead of passing to the other conductor, curves round and returns to the same conductor. Although in recent years the tubular waveguide has made phenomenal progress and become a widely-used piece of apparatus, little use has been made of single-wire transmission. In the May number of the Radio-Electronic Engineering edition of *Radio & Television News* there is an article with the above title by Dr. Goubau of the American Signal Corps Engineering Laboratories, in which he describes some experiments made with such a transmission system.

Fig. 1 is a reproduction of Fig. 1 of our 1936 Editorial; it shows how the electric flux, which, in the presence of an outer conductor, would have been radial, curves round and returns to the conductor. An interesting question now arises as to the distribution of this field; how far do the electric lines of force extend before they curve round and return? As Dr. Goubau points out, it is important to keep the field as close as possible to the wire, both to avoid interference and as we shall see, to obtain a high efficiency of transmission. It is shown that the radial extent of the wave depends very largely on the phase velocity; a small decrease in the phase

velocity, and therefore in the wavelength on the wire, causes an increased concentration of the field in the neighbourhood of the wire. The phase velocity will be reduced slightly by the resistivity of the conductor; at the frequencies employed skin effect will be very pronounced. The author also states that cutting a screw thread on the wire causes an appreciable reduction of the phase velocity; for the very thin effective conducting layer, the corrugation will lengthen the actual path of the surface currents. The method mainly employed, however, consists in coating the wire with enamel; even if the wire were a perfect conductor, a coating of enamel would cause a decrease in the phase velocity and a consequent spatial limitation of the field.

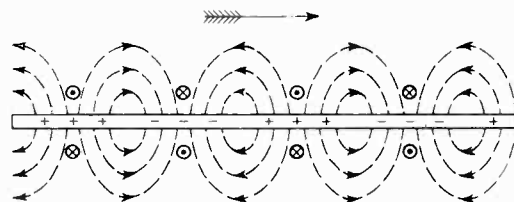


Fig. 1

The method employed by the author for setting up the wave consists in terminating the outer conductor of a coaxial cable in a funnel-shaped horn, while the inner conductor is continued as the transmission line. A similar horn at the receiving end collects the wave and carries it into a coaxial cable. This is illustrated in Fig. 2. The diameter of the mouth of the horn was 13 inches (not 13 feet as indicated in his diagram). Experiments were made with a 2-mm copper wire 120 ft long at frequencies of 1 600, 3 300, and 4 700 Mc/s. The author claims that the waves can be passed from the coaxial cable to the single line by means of the horn with a loss of only 10 per cent, but

the appropriate size of horn will depend on the wavelength. Unless the field is confined to the immediate neighbourhood of the wire, some of it will fail to pass into the collecting horn and thus reduce the efficiency. By the reciprocity

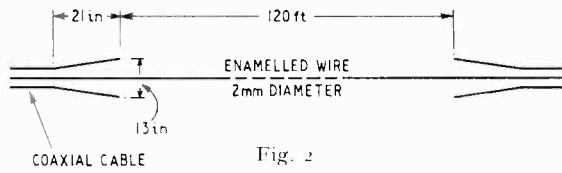


Fig. 2

theorem the same will be true at the transmitting horn. Fig. 3 shows the losses in decibels for the 120-ft line. In the calculations the enamel was assumed to have a dielectric constant of 3, a power-factor of 0.008, and a thickness of 0.05 mm. L_c , L_h and L_i are the losses in the conductor, horns, and insulation respectively; L_{tot} is the total loss. It is stated that the losses in the same length of a very good cable at the same frequencies are from 6 to 10 times as great. It will be seen that the losses in the horns increase rapidly with the wavelength. Fig. 4 shows how the losses vary with the thickness of the dielectric coating. These curves are, we understand, based on calculations, but have been verified experimentally.

Particulars are given of another very striking experiment. Tests were made at a frequency of 2 600 Mc/s on an outdoor copper wire 2.6 mm diameter 120 ft long with the same horns as before. Having been outside for some months the wire was corroded, but on cleaning it with sandpaper the loss went up from 3 to 3.6 db; perhaps this is not surprising if the efficiency

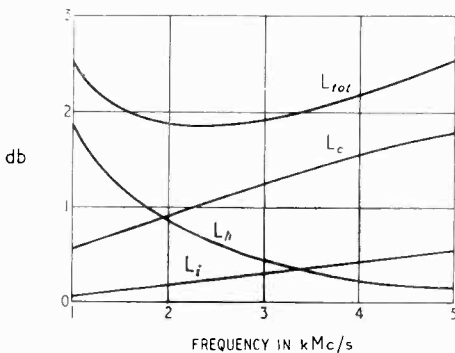


Fig. 3

can be increased by cutting a screw-thread on the wire. The wire was then given several coats of polystyrene solution, and the loss went down more and more until it reached a minimum of 1.7 db, but on adding further coats it went up to 1.9 db. The thickness was too variable for any value of the average thickness to be

given. As we mentioned at the beginning the line can be either a conductor or a dielectric, and the results of these experiments seem to indicate that the layer of dielectric plays an important part in the transmission. It is true that it is very thin, but due to skin effect, the effective thickness of the conducting layer of the copper wire, at the frequencies employed is only about a thousandth of a millimetre, so that the transmission line may be regarded as a polystyrene cylinder with a metal lining.

Tests were also made on a 600 ft line of 3.2 mm copper wire with a layer of enamel 0.25 mm thick. The distance from the ground varied between 4 and 8 feet, and the wire was supported every 80 feet by waxed strings. The measured loss at 1 600 Mc/s was 5 db whereas the same length of a very good cable has an attenuation of 70 db. The effect of rain was investigated; a uniform film of water did not increase the loss, but rows of big rain drops did, the maximum increase being 1.5 db.

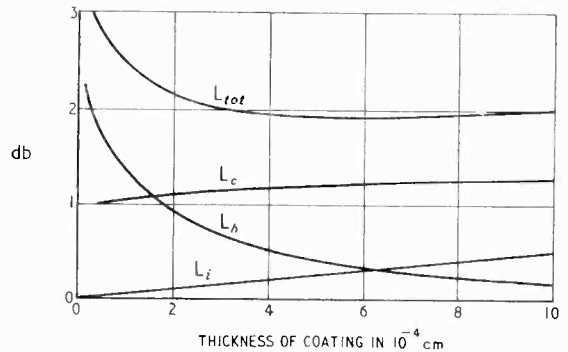


Fig. 4

The article does not show how the calculated results were arrived at, nor does it discuss in detail the phenomena involved. This will doubtless follow.

The discussion of this type of transmission in Stratton's "Electromagnetic Theory" shows that one cannot go far without becoming involved in very complex mathematics. The field distribution and the energy involved do not lend themselves to simple calculation, but the striking experimental results obtained by Dr. Goubau show that it is a subject that must be fully investigated.

G. W. O. H.

A slight reduction in the number of pages in *Wireless Engineer*, and some delay in publication, are still unavoidable on account of the continued withdrawal of overtime working by a section of the printing industry. All journals printed in London are similarly affected, to a greater or lesser extent, but journals printed in the provinces are unaffected.

SIMPLE WAVE ANALYSER

By **D. Martineau Tombs, M.Sc., A.C.G.I., D.I.C., A.M.I.E.E.**

(Dept. of Electrical Engineering, Imperial College)

SUMMARY.—The device, in principle, uses the selective property of a simple tuned circuit to isolate a particular component of frequency existing in a complex wave.

The wave to be analysed is displayed on one trace of a double-beam oscilloscope and the selected component on the other. The amplitude of the harmonic being selected is governed by the selectivity (or Q), which can be adjusted over a wide range by the use of a negative-resistor. Under conditions of adequate selectivity, the Q may then be determined by detuning. If, further, the Q s are adjusted successively to make the magnified voltage the same for two harmonics, the ratio of harmonic amplitudes is given by $e_m/e_n = (\omega_m/\omega_n)^2 (\Delta C_m/\Delta C_n)$, where $e_m =$ e.m.f. of the m^{th} harmonic; $e_n =$ e.m.f. of the n^{th} harmonic. The ratio ω_m/ω_n comes from the display, the ratio $\Delta C_m/\Delta C_n$ from the half-power points. The use of a mutual-inductive coupling and a cathode follower extend the usefulness of the analyser.

The apparatus required for such a device is normally available in most laboratories, or can readily be made. The cost is a fraction of that of a commercial wave analyser.

Introduction

THE circuit of Fig. 3 shows the essential parts of an early form of analyser. Its performance may best be described by reducing the network to an equivalent circuit. Thus, referring to Fig. 1(a), it will be seen that the analyser is basically a simple tuned circuit consisting of a fixed linear inductor L , the inductance of which is supposed constant in value (or known) over the frequency range covered by the analyser, a variable capacitor C , having a known incremental calibration, and which, with the inductor, allows tuning over the frequency range. e represents the e.m.f. of the unbalanced source to be analysed, and E_n the r.m.s. value of the magnified (or selected) voltage.

The process of analysis consists in deducing in turn the r.m.s. value of each component, e_n , present in the complex wave, measurement being made in the presence of all other components. This selection is done by reducing the effective series resistance R until E_n is purely sinusoidal, then measuring E_n and the magnification, from which e_n may be deduced.

The theory will be briefly stated on the assumption, which will be justified later, that adequate selectivity can be produced.

Theory

First consider the circuit of Fig. 1(a) tuned to a particular component e_n , all other components being of negligible amplitude. Let E_n be the maximum r.m.s. value of the voltage appearing across the capacitor, then

$$E_n = Qe_n \quad \dots \quad (1)$$

where Q is the magnification (or selectivity) of the circuit.

It is well known that Q , for reasonably high values, may be determined by detuning. If the capacitor is detuned by $\pm \Delta C/2$ from its tuned value C_r until E_n drops to $E_n/\sqrt{2}$

$$\text{then } Q = 2C_r/\Delta C \quad \dots \quad (2)$$

From (1) and (2)

$$e_n = \frac{\Delta C}{2C_r} E_n \quad \dots \quad (3)$$

And since at resonance

$$C_r = 1/\omega^2 L \quad \dots \quad (4)$$

$$\text{then } e_n = \frac{\Delta C}{2} \omega^2 L E_n \quad \dots \quad (5)$$

This is the basic equation for the equivalent circuit. It may be extended to cover the circuit of Fig. 1(c). Let Y denote the unilateral transfer admittance of the cathode follower, and M the mutual inductance between the small coil (in practice a few turns) in the cathode of the follower and the coil of the resonant circuit. If Y be regarded as constant over the range of harmonic frequency involved, it is given by i_n/V_n for each harmonic; or in general

$$Y = I/V \quad \dots \quad (6)$$

$$\text{thus } V_n = \frac{\Delta C}{2} \omega \frac{1}{Y M} E_n \quad \dots \quad (7)$$

The advantage of the magnetic coupling is that the induced e.m.f. increases with frequency, and this tends to offset the reduced amplitude of the higher-order harmonics that are usually encountered in practice.

The introduction of the cathode follower makes the input impedance of the device large, and its unilateral property isolates the source from the highly-selective tuned circuit. Harmonic distortion due to non-linearity appears to be negligible in practice, as may be verified by a current analysis using the circuit of Fig. 1(b) with and without the cathode follower in circuit.

Selectivity

In deriving the above equations it has been assumed that all harmonics except the one being studied have been sufficiently attenuated. This has implied an adequate selectivity in the resonant circuit.

MS accepted by the Editor, December 1949

Such a performance can be realized by the application to the circuit of one of a variety of known active networks. In the first models of the analyser a tetrode valve adjusted to the region of its negative slope was employed (Fig. 3), control being obtained by a variable resistor R_0 in the cathode.

be the true one, will be reached. Thus e_n of Fig. 1(a), i_n of Fig. 1(b) or v_n of Fig. 1(c) are accurately determined.

Nevertheless, by examining the waveforms to be expected from an adjustment with insufficient selectivity, it may be shown that if n is the order of harmonic tuned to, and m the

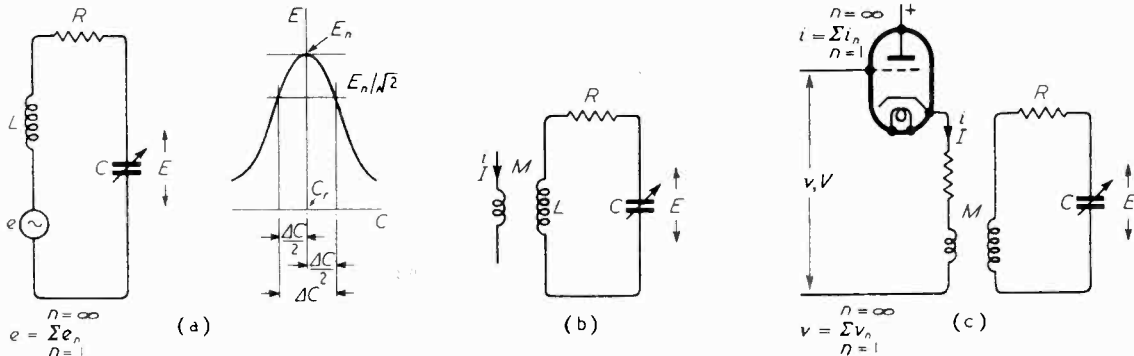


Fig. 1. The equivalent circuits of simple types of analyser: (a) source e being analysed; (b) source I being analysed; (c) source V being analysed.

Provided the amplitude of swing along the anode characteristic of the tetrode is maintained small (one volt r.m.s. in this case) the behaviour of the valve may be considered linear, and represented by a single symbol r^* (Fig. 2.)

The effective selectivity Q of the circuit shown in this figure may be calculated by considering the LC circuit (the dynamic impedance Z of which at its anti-resonant frequency is L/CR_0) is in parallel with r . Thus for the circuit of Fig. 2

$$Q = \frac{I}{\omega L} \left[\frac{Z}{I + Z/r} \right] \dots \dots \dots (8)$$

As r is reduced from a high initial negative value, Q increases continuously. Stable values of several hundred may be realized at frequencies as low as a few hundred cycles per second, and it is not difficult in practice to satisfy the requirement of adequate reduction of all other harmonic components relative to the one under consideration. Instability occurs when r becomes less in magnitude than Z .

order interfering (or breaking through), then the peaks of the displayed wave will be non-uniform in height if $m < n$ and also for all values of $m > n$ except $m = (2, 3, 4 \dots) n$. Thus, if the third harmonic were tuned to ($n = 3$), a strong sixth harmonic ($m = 6$) would not alter the relative height of successive peaks, and thus would constitute a failure of a test for adequate selectivity based on the uniformity of peaks. In practice, however, the test of uniformity of peak

height enables the circuit to be rapidly adjusted to the desired selectivity, the final necessary step being a check at a slightly higher degree of selectivity.

Fig. 2. The addition of a voltage-controlled negative resistance r to reduce the effective losses.

It should be noted that the worst failure occurs with the fundamental, since the presence of harmonics in this case does not alter the magnitude of successive peaks. The difficulty, however, is not as serious as might be supposed, since the fundamental is more widely separated from the second harmonic than any other harmonic from its adjacent one.

Thus, in practice, the first test, and often a sufficient one, is to increase the selectivity until the peaks are of equal height. The second test is to make a further measurement with a greater selectivity. If the results are sufficiently close a third test at still higher selectivity is unnecessary.

* To avoid confusion about signs, the symbol r is taken to mean a resistance of positive or negative value. In this application the dynatron had a minimum value when negative of $r = -23,000 \Omega$.

Fig. 4 shows a series of oscillograms taken using a double-beam oscillograph. The wave being analysed was kept on the upper trace as a reference system, while the tips of the selected harmonic were displayed on the lower trace. The separate oscillograms were taken when adequate selectivity had been reached at each harmonic in turn. It will be noted that not only the amplitudes of different selected harmonics (on different pictures) are adjusted to the same value, but that the individual peak heights of harmonics within the period of a cycle of the fundamental, are also made the same. The technique of doing this is described later.

It may be objected that on close examination of the harmonic trace, particularly of the right-hand group, the individual amplitude of peaks is not constant, indicating insufficient selectivity. This, in fact, is not the case, since the inequality is due to interbeam coupling within the cathode-ray tube itself, a source of error quickly recognized by a reduction of the reference-trace amplitude.

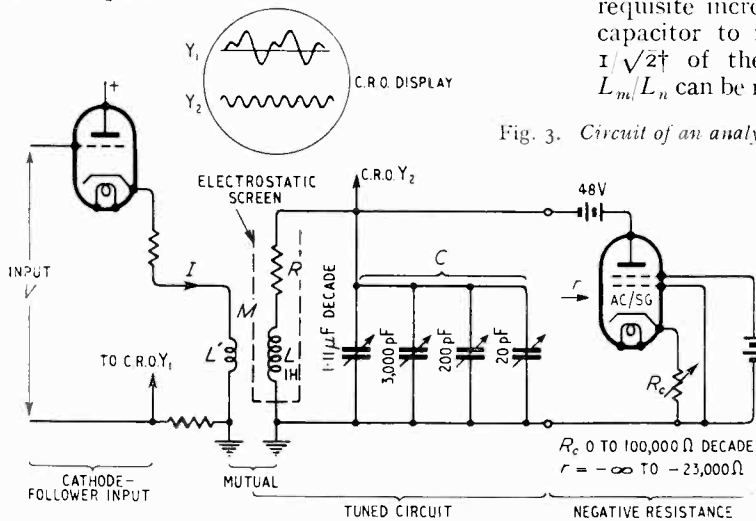


Fig. 3. Circuit of an analyser.

Stability Criteria

Although, in equation (8) it has been considered adequate to take the negative-resistance as linear, at the threshold of oscillation the second-order curvature is of importance if the device is to move smoothly and not discontinuously into and out of oscillation under the control of R_c (Fig. 3). If, for an increasing amplitude of signal about the operating point, "the effective negative-resistance" becomes greater, the circuit is stable, but if the reverse is the case, discontinuous operation occurs, and the amplitude of the display increases indefinitely, no longer under the incremental control of R_c . r must be very greatly increased by increasing R_c and the condition of high selectivity re-approached

slowly by reducing r . This may be given mathematical formulation by stating that if the dynatron characteristic is plotted as $I = f(V)$ the circuit in the region of negative resistance is stable if d^3I/dV^3 is positive and unstable if negative.

If the wave to be analysed is displayed on one trace of a double-beam oscilloscope, and the analysed component on the other, the condition of oscillation is immediately evident from relative movement of the two patterns.

Comparing Harmonics

If two frequency components, m and n , are to be compared in amplitude, then, using equation (7).

$$\frac{V_m}{V_n} = \frac{Y_n E_m \omega_m \Delta C_m L_m M_n}{Y_m E_n \omega_n \Delta C_n L_n M_m} \quad \dots (9)$$

and the analysis is performed when the above series of ratios is determined.

Of these ratios, ω_m/ω_n , comes directly from the display by counting, and $\Delta C_m/\Delta C_n$ from the requisite incremental adjustments of the tuning capacitor to reduce E_m and E_n respectively to $1/\sqrt{2}$ † of their resonant values. Y_m/Y_n and L_m/L_n can be made very close to unity. Likewise

E_m/E_n may be made unity in two ways, as follows: if a standard mutual inductance is available, the calibration of which is valid over the frequency range, convenient known values of M may be used for the different harmonics. By such means E_m may be made equal to E_n , leaving the ratio $M_n/M_m = 1$, and E_m and E_n made equal by suitable use of the variable negative resistance r .

As discussed above r must be adjusted to give at least sufficient selectivity, but there is no objection to increasing the selectivity further, where necessary. This freedom to increase the selectivity allows the observed value of E on the oscilloscope to be varied arbitrarily. A convenient technique is to choose a suitable amplitude on the oscilloscope and adjust the selected harmonics in turn to this value, if necessary returning over earlier measurements which may have to be repeated with a higher degree of selectivity to meet the dual requirements of adequate selectivity and equality of E_m and E_n . It is obviously undesirable to use a greater degree of selectivity

† Or to any other convenient ratio.

than is necessary since the circuit is proceeding towards instability.

A direct, though approximate, measure of the actual value of E is given from the oscilloscope trace, but the measure may be obtained alternatively by use of a valve voltmeter, provided care is taken to ensure that the input impedance of the voltmeter does not introduce errors at high Q values.† The advantage of adjusting the deflection to a constant value avoids the need of a calibrated instrument.

Experimental Results

In Table 1 the results of comparative analysis as carried out by the method described, and by the use of a good commercial analyser, are shown. In this case the source being examined was a fork-controlled oscillator. A high degree of frequency stability is essential if very selective circuits are to be employed. Fig. 4 shows a series of oscillograms taken during a test, and employing the technique of the previous section.

TABLE 1

Harmonic Number n	Author's Analyser		Commercial Analyser
	ωC_n (ρF) between the two $\frac{1}{2}$ -power points	Harmonic Ratio $n \frac{\Delta C_n}{\Delta C_1} = 100\%$	Harmonic Ratio %
1	14,000	100	100
2	910	13.0	13.7
3	721	15.4	16.3
4	210	6.0	6.0
5	103	3.80	4.0
6	54.6	2.3	2.4
7	not measured		
8			
9	6.56	0.42	0.4

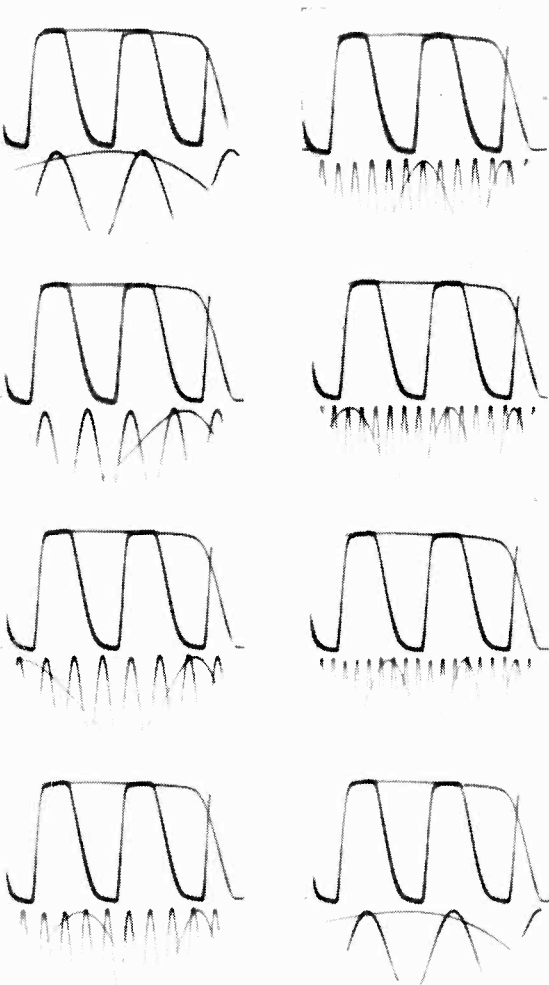


Fig. 4. A series of harmonics recorded during a test. The upper trace is of the wave being analysed, while the lower trace shows the peaks of selected harmonics.

Stray Fields

It is surprising at first, in using these highly-selective circuits, to find how sensitive they are to stray fields in a laboratory. Tuning to the seventh harmonic of the mains and moving the coil L into different positions, the field pattern both in magnitude and direction, due to a piece of mains-operated apparatus can readily be mapped. It is also helpful for demonstration purposes to couple the output of the selected harmonic on to a loud-speaker, thus facilitating the exploration of stray fields where the oscilloscope may not be visible.

The apparatus substantially as described herein, was exhibited at the Centenary Celebrations at Imperial College in November 1945, and subsequently at the Physical Society's Exhibition in January 1946. Since then, W. I. Heath and J. A. Fredericks, at the General Electric Research Laboratories, Wembley, England, have made a mains-operated analyser dependent on the above principle. The first G.E.C. model was shown at the Physical Society's Exhibition in April 1949, on the author's stand.

Acknowledgment

The author wishes to thank Professor Willis Jackson and Mr. M. F. McKenna for helpful criticism in the preparation of the paper.

† The dynamic impedance of the circuit at such values may be several megohms, and is directly given by $Z = 2(\omega \Delta C)$. This provides a convenient method of measuring the input impedance of such devices.

NEGATIVE-FEEDBACK AMPLIFIERS

Conditions for Critical Damping

By J. E. Flood, B.Sc. (Eng.)

I. Introduction

WHEN negative feedback is applied to a resistance-coupled amplifier having two or more stages it is well-known that, once a certain amount of feedback is exceeded, the frequency characteristic develops peaks at the edges of the band and the transient response of the amplifier contains a damped oscillation. Brockelsby¹ and Mayr² have shown that a substantially flat response over the maximum possible frequency band can be obtained by arranging for a suitable relationship between the time constants of the stages of the amplifier. The condition of maximal flatness, however, still gives an oscillatory transient response: for instance, when the input voltage is a unit step (i.e., a voltage which is zero when $t < 0$ and unity when $t > 0$) the two-stage maximally-flat amplifier has a response which overshoots 4.3%, and the three-stage amplifier overshoots 8%.

The present analysis determines the relationship required between the time constants of a two-stage amplifier with a feedback path whose transfer coefficient β is independent of frequency in order to obtain the most rapid transient response which is possible without overshoot; this corresponds to the condition of critical damping. It is shown that a modification of the feedback path enables a critically-damped response to be obtained when the ratio between the time constants of the stages is less than that required for critical damping when β is independent of frequency. It is shown that a critically-damped transient response can also be obtained from a three-stage amplifier by modifying the feedback path.

The effective feedback of the amplifier decreases at high frequencies and at the high-frequency end of the band there is little or no feedback. The amplifier is therefore unsuitable for a multichannel carrier-system amplifier, but is suitable for video-frequency or pulse amplification. The steady-state gain of the amplifier is stabilized by the full amount of the feedback at low frequencies; the feedback at the higher frequencies only ensures that the bandwidth is adequate for a sufficiently rapid transient response and that the shape of the frequency-response curve is such that the transient response is free from ringing. The analysis assumes that

the operation of the amplifier is linear. It is important that a signal shall not be applied to the amplifier which rises to sufficient magnitude to overload the amplifier before the voltage feedback has built up to its steady-state value.

2. Indicial Response of Feedback Amplifiers

If the Heaviside operational expression for the indicial response (i.e., the response to a unit step) of an amplifier is $\mu(p)\mathbf{1}$, and the input voltage is $e(t)\mathbf{1}$, the output voltage is

$$\mu(p) \cdot e(t)\mathbf{1}$$

Let the indicial response of the feedback path be $\beta(p)\mathbf{1}$, so that the voltage returned to the input circuit to produce feedback is

$$\mu(p) \cdot \beta(p) \cdot e(t)\mathbf{1}$$

If the input voltage to the feedback amplifier is a unit step, then

$$e(t)\mathbf{1} = \mathbf{1} - \mu(p) \cdot \beta(p) \cdot e(t)\mathbf{1}$$

$$\therefore e(t)\mathbf{1} = \frac{\mathbf{1}}{\mathbf{1} + \mu(p) \cdot \beta(p)} \mathbf{1}$$

\therefore The output voltage is

$$h(p)\mathbf{1} = \frac{\mu(p)}{\mathbf{1} + \mu(p) \cdot \beta(p)} \mathbf{1} \quad \dots \quad (1)$$

which is the indicial response of the feedback amplifier. The sign convention is chosen so that μ and β are both positive quantities when the feedback is negative.

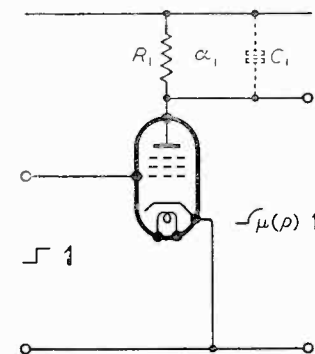


Fig. 1. Basic RC amplifier circuit.

3. Single-stage Amplifier

The type of amplifier considered is shown in Fig. 1. The anode load resistance is R_1 and C_1 is the total stray capacitance. If the steady-state low-frequency gain of the amplifier without feedback is μ_0 , its indicial response is

$$\mu(p)\mathbf{1} = \mu_0 \frac{\alpha_1}{p + \alpha_1} \mathbf{1} = \mu_0(\mathbf{1} - e^{-\alpha_1 t})\mathbf{1}$$

$$\text{where } \alpha_1 = \mathbf{1}/R_1C_1$$

MS accepted by the Editor, January 1950

If the transfer coefficient of the feedback path is β_0 and is independent of frequency, the indicial response of the amplifier with feedback is

$$\begin{aligned}
 h(p)\mathbf{1} &= \frac{\mu_0 \frac{\alpha_1}{p + \alpha_1}}{\mathbf{1} + \mu_0 \beta_0 \frac{\alpha_1}{p + \alpha_1}} \mathbf{1} \\
 &= \frac{\mu_0 \alpha_1}{p + \alpha_1 (\mathbf{1} + \mu_0 \beta_0)} \mathbf{1} \\
 &= \frac{\mu_0}{\mathbf{1} + \mu_0 \beta_0} \cdot \frac{\alpha}{p + \alpha} \mathbf{1} \quad \dots \dots (2)
 \end{aligned}$$

where $\alpha = \alpha_1 (\mathbf{1} + \mu_0 \beta_0)$

$$\therefore h(t) = \frac{\mu_0}{\mathbf{1} + \mu_0 \beta_0} (\mathbf{1} - e^{-\alpha t}), \quad t > 0 \quad \dots (3)$$

The feedback reduces the time constant of the amplifier in the same ratio as it reduces the gain at low frequencies. The steady-state gain is stabilized by the feedback so that if $\mu_0 \beta_0 \gg \mathbf{1}$, it will remain almost constant when the gain of the stage decreases (e.g., due to valve aging), but the time-constant of the circuit increases as the gain decreases. In order to obtain a stable gain under pulse conditions it is therefore necessary that the time-constant with feedback shall be sufficiently small for the pulse response to reach substantially steady-state when the gain is the smallest value likely to be encountered in practice.

4. Two-stage Amplifier

Fig. 2 shows a typical two-stage amplifier and the three-stage amplifier shown in Fig. 3 also contains two time-constants within the feedback loop.

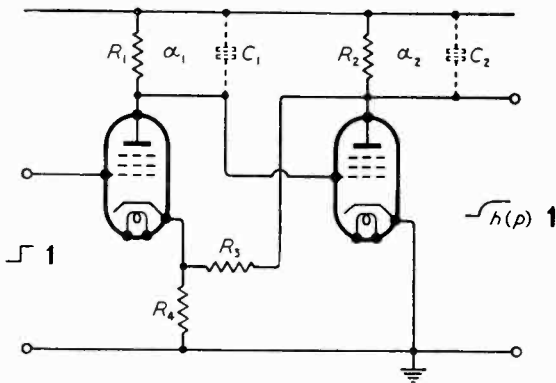


Fig. 2. Two-stage feedback amplifier.

The indicial response of the amplifying path is

$$\begin{aligned}
 \mu(p)\mathbf{1} &= \mu_0 \frac{\alpha_1}{p + \alpha_1} \cdot \frac{\alpha_2}{p + \alpha_2} \mathbf{1} \quad \dots \dots (4) \\
 \text{where } \alpha_1 &= \mathbf{1}/R_1 C_1 \quad \text{and} \quad \alpha_2 = \mathbf{1}/R_2 C_2.
 \end{aligned}$$

The indicial response with feedback (the transfer coefficient being β_0 and independent of frequency) becomes

$$\begin{aligned}
 \bar{h}(p)\mathbf{1} &= \frac{\mu_0 \frac{\alpha_1}{p + \alpha_1} \cdot \frac{\alpha_2}{p + \alpha_2}}{\mathbf{1} + \mu_0 \beta_0 \frac{\alpha_1}{p + \alpha_1} \cdot \frac{\alpha_2}{p + \alpha_2}} \mathbf{1} \\
 &= \frac{\mu_0 \alpha_1 \alpha_2}{p^2 + p(\alpha_1 + \alpha_2) + \alpha_1 \alpha_2 (\mathbf{1} + \mu_0 \beta_0)} \mathbf{1} \quad \dots \dots (5) \\
 &= \frac{\mu_0 \alpha_1 \alpha_2}{(p + \lambda_1)(p + \lambda_2)} \mathbf{1}
 \end{aligned}$$

where $(p + \lambda_1)$, $(p + \lambda_2)$ are the factors of the denominator of equation (5). If λ_1 , λ_2 are complex, the response is of the form

$$h(t) = \mathbf{1} - A e^{-\alpha t} \sin(\omega t + \phi) \quad \dots \dots (6)$$

which represents a damped oscillation.

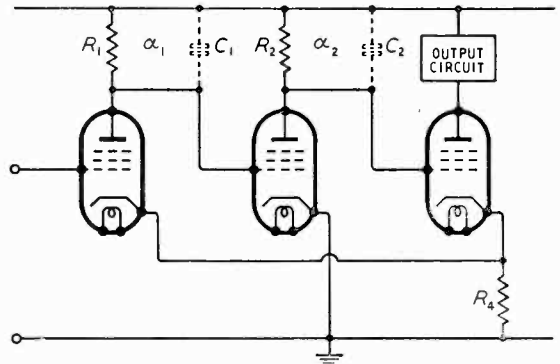


Fig. 3. Three-stage feedback amplifier with only two time constants within the feedback loop.

If λ_1 , λ_2 are real, but unequal, the response is of the form

$$h(t) = \mathbf{1} - B e^{-\alpha t} \sinh(\beta t + \gamma) \quad \dots \dots (7)$$

which is aperiodic.

If $\lambda_1 = \lambda_2 = \alpha$, the response is of the form

$$h(t) = \mathbf{1} - (\mathbf{1} + \alpha t) e^{-\alpha t} \quad \dots \dots (8)$$

which corresponds to critical damping and gives the quickest build-up which is possible without overshoot. Now

$$\begin{aligned}
 \lambda_1, \lambda_2 &= \frac{1}{2} \{ (\alpha_1 + \alpha_2) \mp \\
 &\quad \sqrt{(\alpha_1 + \alpha_2)^2 - 4\alpha_1 \alpha_2 (\mathbf{1} + \mu_0 \beta_0)} \}
 \end{aligned}$$

\therefore In order to ensure real factors

$$\mathbf{1} + \mu_0 \beta_0 \leq \frac{(\alpha_1 + \alpha_2)^2}{4\alpha_1 \alpha_2}$$

$$\text{and when } \mathbf{1} + \mu_0 \beta_0 = \frac{(\alpha_1 + \alpha_2)^2}{4\alpha_1 \alpha_2},$$

the factors are equal and the overall indicial response is

$$h(p)\mathbf{1} = \frac{\mu_0 \alpha_1 \alpha_2}{(p + \alpha)^2} \mathbf{1}$$

$$= \frac{\mu_0}{1 + \mu_0 \beta_0} \cdot \frac{\alpha^2}{(p + \alpha)^2} \mathbf{1} \quad \dots \quad (9)$$

where

$$\alpha = \frac{1}{2}(\alpha_1 + \alpha_2) = \sqrt{\alpha_1 \alpha_2 (1 + \mu_0 \beta_0)} \quad \dots \quad (10)$$

$$\therefore h(t) = \frac{\mu_0}{1 + \mu_0 \beta_0} [1 - e^{-\alpha t} (1 + \alpha t)], t > 0 \quad \dots \quad (11)$$

Fig. 4 shows the feedback factor $(1 + \mu_0 \beta_0)$ and the resulting time constant plotted against the ratio of the time constants of the two stages. If a large amount of feedback is to be used, the ratio of the time constants must be large.

The condition for maximal flatness (a term introduced by Landon³) is given by Brockelsby¹ as

$$F = 2S^2$$

where

$$F = (1 + \mu_0 \beta_0) \quad \text{and} \quad S = \frac{\alpha_1 + \alpha_2}{2\sqrt{\alpha_1 \alpha_2}}$$

$$\therefore 1 + \mu_0 \beta_0 = \frac{(\alpha_1 + \alpha_2)^2}{2\alpha_1 \alpha_2}$$

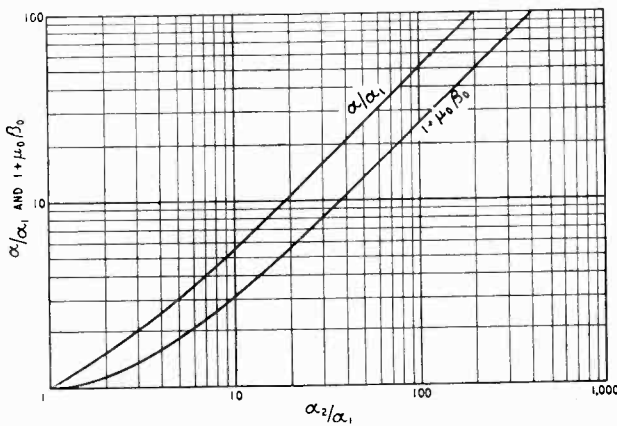


Fig. 4. Conditions for critical damping of two-stage uncompensated amplifier.

It is seen that for any particular ratio of α_2/α_1 , the condition of critical damping permits a feedback factor of only one-half that required for maximal flatness of the frequency characteristic. The transient response of the maximally-flat amplifier is therefore oscillatory.

More feedback can be obtained by modifying the feedback path so that its indicial response is

$$\beta_0 \frac{p + \alpha_3}{\alpha_3} \mathbf{1}$$

If a capacitance C_3 is connected in parallel with R_3 , as shown in Fig. 5, and $R_3 \gg R_4$, then

$$\beta(p)\mathbf{1} \approx \beta_0 (1 + p C_3 R_3) \mathbf{1}$$

$$= \beta_0 \frac{p + \alpha_3}{\alpha_3} \mathbf{1}$$

where $\alpha_3 = 1/R_3 C_3$

If an inductance L is connected in series with R_4 , as shown in Fig. 6, and $g_m R_4 \ll 1$ then

$$\beta(p)\mathbf{1} \approx \beta_0 \left(1 + p \frac{L}{R_4}\right) \mathbf{1}$$

$$= \beta_0 \frac{p + \alpha_3}{\alpha_3} \mathbf{1}$$

where $\alpha_3 = R_4/L$.

The indicial response $\frac{p + \alpha_3}{\alpha_3} \mathbf{1}$ corresponds to

an amplitude characteristic which rises with frequency and becomes infinite at infinite frequency. The amplitude characteristics of the β paths of Figs. 5 and 6 cannot rise above unity, but the circuits approximate sufficiently well to the required response provided that $R_3 \gg R_4$ and $g_m R_4 \ll 1$.

The overall indicial response is

$$h(p)\mathbf{1} = \frac{\mu_0 \frac{\alpha_1}{p + \alpha_1} \cdot \frac{\alpha_2}{p + \alpha_2}}{1 + \mu_0 \beta_0 \frac{\alpha_1}{p + \alpha_1} \cdot \frac{\alpha_2}{p + \alpha_2} \cdot \frac{p + \alpha_3}{\alpha_3}} \mathbf{1}$$

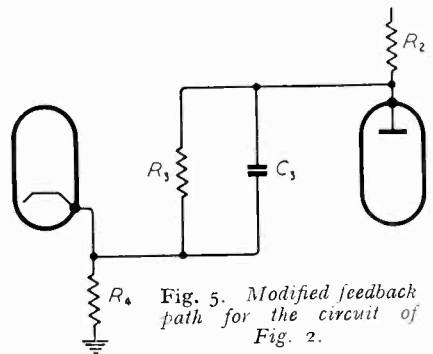


Fig. 5. Modified feedback path for the circuit of Fig. 2.

$$= \frac{\mu_0 \alpha_1 \alpha_2}{p^2 + p \left(\alpha_1 + \alpha_2 + \frac{\alpha_1 \alpha_2}{\alpha_3} \mu_0 \beta_0 \right) + \alpha_1 \alpha_2 (1 + \mu_0 \beta_0)} \mathbf{1} \quad \dots \quad (12)$$

The factors of the denominator are

$$(p + \lambda_1), (p + \lambda_2)$$

where

$$\lambda_1, \lambda_2 = \frac{1}{2} \left\{ \left(\alpha_1 + \alpha_2 + \frac{\alpha_1 \alpha_2}{\alpha_3} \mu_0 \beta_0 \right) \mp \right.$$

$$\left. \sqrt{\left(\alpha_1 + \alpha_2 + \frac{\alpha_1 \alpha_2}{\alpha_3} \mu_0 \beta_0 \right)^2 - 4\alpha_1 \alpha_2 (1 + \mu_0 \beta_0)} \right\}$$

If the factors are equal,

$$\alpha_3 = \frac{\alpha_1 \alpha_2 \mu_0 \beta_0}{2\sqrt{\alpha_1 \alpha_2 (\Gamma + \mu_0 \beta_0)} - (\alpha_1 + \alpha_2)} \dots (I3)$$

and

$$h(p) \mathbf{1} = \frac{\mu_0 \alpha_1 \alpha_2}{(p + \alpha)^2} \mathbf{1} = \frac{\mu_0}{\Gamma + \mu_0 \beta_0} \cdot \frac{\alpha^2}{(p + \alpha)^2} \mathbf{1} \quad (9)$$

where

$$\alpha = \sqrt{\alpha_1 \alpha_2 (\Gamma + \mu_0 \beta_0)} \dots \dots \dots (I4)$$

$$\therefore h(t) = \frac{\mu_0}{\Gamma + \mu_0 \beta_0} [\Gamma - e^{-\alpha t} (\Gamma + \alpha t)], t > 0 \dots (I1)$$

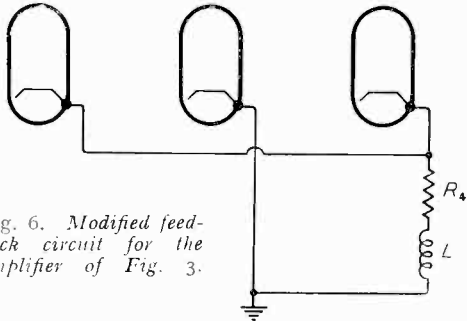


Fig. 6. Modified feedback circuit for the amplifier of Fig. 3.

By the choice of the value given by equation (I3) for the time constant for the feedback circuit, critical damping is obtained and the indicial response of the feedback amplifier is made identical with that of an amplifier without feedback having two stages, each having a time constant equal to the geometric mean of the time constants of the two stages multiplied by the square root of the feedback factor. A particularly simple special case is obtained when $\alpha_2 = \alpha_1 (\Gamma + \mu_0 \beta_0)$, then $\alpha = \alpha_3 = \alpha_2 = \alpha_1 (\Gamma + \mu_0 \beta_0)$.

If the time constant of the anode load of the third stage of the amplifier of Fig. 3 is also made Γ/α , the indicial response of the three-stage amplifier is

$$h(p) \mathbf{1} = \frac{\mu_0}{\Gamma + \mu_0 \beta_0} \cdot \frac{\alpha^3}{(p + \alpha)^3} \mathbf{1} \dots \dots (I5)$$

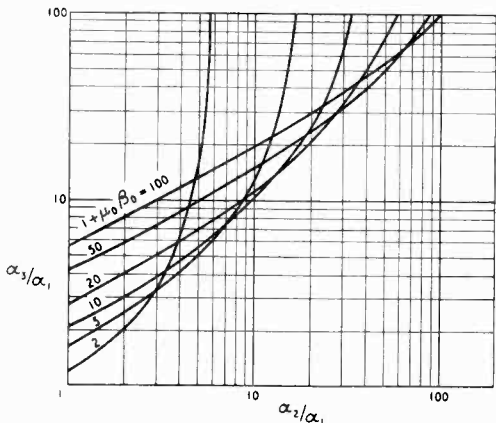


Fig. 7. Conditions for critical damping of two-stage compensated amplifier.

$$\therefore h(t) = \frac{\mu_0}{\Gamma + \mu_0 \beta_0} \left[\Gamma - e^{-\alpha t} \left(\Gamma + \alpha t + \frac{\alpha^2 t^2}{2} \right) \right], t > 0 \dots (I6)$$

Figs. 7 and 8 show the variation of the time constant of the amplifier and of the feedback path plotted against the ratio between the time constants of the two stages for different values of $\Gamma + \mu_0 \beta_0$. Both α and α_3 increase with an increase in this ratio until

$$\Gamma + \mu_0 \beta_0 = \frac{(\alpha_1 + \alpha_2)^2}{4\alpha_1 \alpha_2}$$

when the time constant of the feedback path is zero. Any further increase in the ratio α_2/α_1 results in the amplifier having an overdamped response of the form of equation (7). If an increase is made in the gain μ_0 of an amplifier which is critically-damped, the transient response will become oscillatory, and if the gain is reduced the response will become overdamped and less rapid.

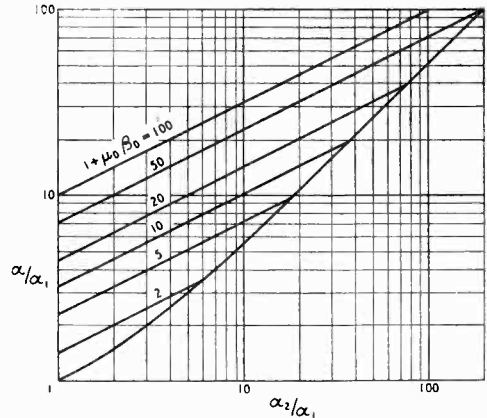


Fig. 8. Time-constant of critically-damped two-stage compensated amplifier.

It is interesting to examine the frequency characteristics of the two-stage amplifier circuit. Fig. 9 shows the amplitude and phase characteristics of an amplifier having the time constant of one stage ten times that of the other. Fig. 10 shows the corresponding Nyquist diagram when there is 26-db of feedback at low frequencies. When the locus of $\mu\beta$ is within the unit circle centre $(-1, 0)$ the feedback has become positive⁴. Although at frequencies at which the feedback is positive, the gain of the μ path has fallen, the net result is a peak in the overall amplitude characteristic which is shown in Fig. 11.

In order to avoid this undesirable rise in the amplitude characteristic, it is necessary to reduce the phase angle of $\mu\beta$ at high frequencies. The vertical line AA' on the Nyquist diagram is the locus for constant gain⁴ and it is undesirable that the locus of $\mu\beta$ could cross this line. A

simple method of reducing the phase shift at high frequencies is to modify the feedback path of the amplifier as shown in Figs. 5 and 6.

Fig. 11 also shows as a broken line the amplitude characteristic of the amplifier when the feedback path is modified to give critical damping ($\alpha_3 = 1.16\alpha_2$). Fig. 10 shows as a broken line the Nyquist diagram corresponding to critical

the overall gain-frequency characteristic is below that of the μ path at all frequencies and the locus of $\mu\beta$ is entirely outside the unit circle centre $(-1, 0)$, touching it at infinite frequency; i.e., the feedback is negative at all frequencies.

If $1 + \mu_0\beta_0 < \frac{\alpha_1^2 + \alpha_2^2}{2\alpha_1\alpha_2}$ the overall gain-frequency

characteristic cuts that of the μ path and is above it at high frequencies, and the locus of $\mu\beta$ cuts the unit circle centre $(-1, 0)$ and is within it at high frequencies; i.e., the feedback is positive at high frequencies. In particular, if β is independent of frequency the critically-damped amplifier has positive feedback at high frequencies and if $\alpha_1 = \alpha_2$ the feedback is always negative. For the example discussed above ($\alpha_2 = 10\alpha_1$, $\mu_0\beta_0 = 20$), when the amplifier is critically damped the feedback is negative at all frequencies, as shown by Figs. 10 and 11.

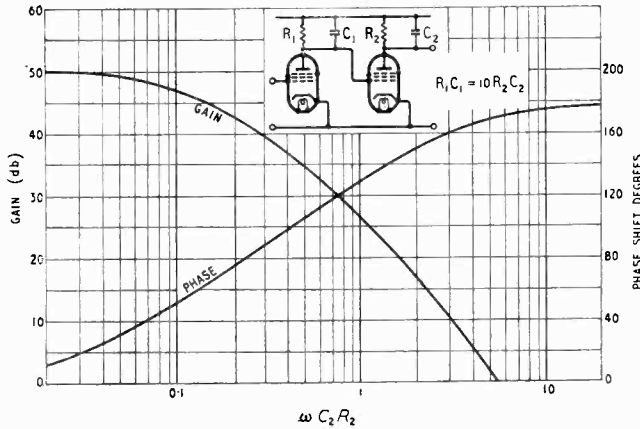


Fig. 9. Amplitude and phase characteristic of two-stage amplifier with one time constant 10 times the other.

damping and shows the large increase in the phase margin⁵ which has resulted.

The gain of the amplifier without feedback is, from equation (4)

$$\mu(\omega) = \mu_0 \frac{\alpha_1 \alpha_2}{(\alpha_1 + j\omega)(\alpha_2 + j\omega)}$$

$$\therefore |\mu(\omega)| = \mu_0 \frac{\alpha_1 \alpha_2}{\sqrt{\alpha_1^2 \alpha_2^2 + \omega^2(\alpha_1^2 + \alpha_2^2) + \omega^4}}$$

The overall gain of the critically-damped feedback amplifier is, from equation (9)

$$A(\omega) = \frac{\mu_0}{1 + \mu_0\beta_0} \cdot \frac{\alpha^2}{(\alpha + j\omega)^2} = \frac{\mu_0 \alpha_1 \alpha_2}{(\alpha + j\omega)^2}$$

where $\alpha = \sqrt{\alpha_1 \alpha_2 (1 + \mu_0\beta_0)}$

$$\therefore |A(\omega)| = \frac{\mu_0 \alpha_1 \alpha_2}{\alpha_2 + \omega^2}$$

At low frequencies $|A(\omega)| = \frac{1}{1 + \mu_0\beta_0} |\mu(\omega)|$

and at high frequencies $|A(\omega)| \approx \frac{\mu_0 \alpha_1 \alpha_2}{\omega^2} \approx |\mu(\omega)|$,

therefore the overall gain-frequency characteristic of the critically-damped amplifier is below that of its μ path at low frequencies and asymptotic to it at high frequencies. It can be simply shown that if

$$1 + \mu_0\beta_0 \geq \frac{\alpha_1^2 + \alpha_2^2}{2\alpha_1\alpha_2}$$

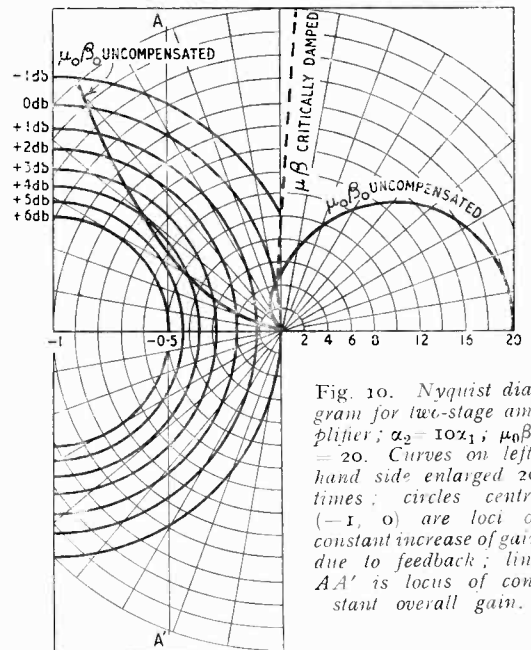


Fig. 10. Nyquist diagram for two-stage amplifier; $\alpha_2 = 10\alpha_1$; $\mu_0\beta_0 = 20$. Curves on left-hand side enlarged 20 times; circles centre $(-1, 0)$ are loci of constant increase of gain due to feedback; line AA' is locus of constant overall gain.

5. Three-stage Amplifier

If an amplifier has three stages with time constants $1/\alpha_1$, $1/\alpha_2$, $1/\alpha_3$ its indicial response is

$$\mu(p) \mathbf{1} = \mu_0 \frac{\alpha_1}{p + \alpha_1} \cdot \frac{\alpha_2}{p + \alpha_2} \cdot \frac{\alpha_3}{p + \alpha_3} \mathbf{1} \quad (17)$$

Let the indicial response of the feedback path be

$$\beta_0(1 + Bp + Ap^2) \mathbf{1}$$

then the indicial response of the amplifier with feedback is

$$h(p)I = \frac{\mu_0 \alpha_1 \alpha_2 \alpha_3}{(p + \alpha_1)(p + \alpha_2)(p + \alpha_3) + \alpha_1 \alpha_2 \alpha_3 \mu_0 \beta_0 (I + Bp + Ap^2)} I \quad (18)$$

$$= \frac{\mu_0 \alpha_1 \alpha_2 \alpha_3}{(p + \lambda_1)(p + \lambda_2)(p + \lambda_3)} I \quad (19)$$

Where

$$(p + \lambda_1), (p + \lambda_2), (p + \lambda_3)$$

are the factors of the denominator of Equ. (18).

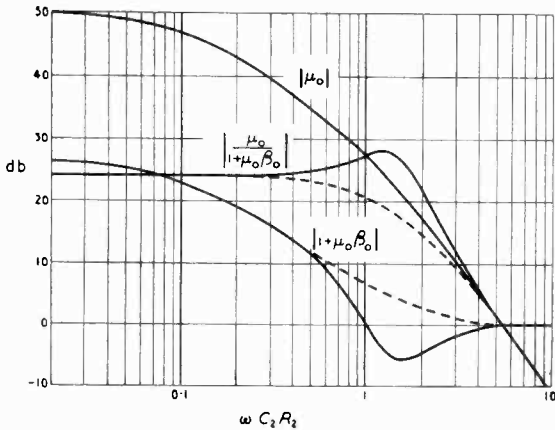


Fig. 11. Amplitude characteristics of two-stage amplifier uncompensated (full line) and critically damped (dashed line).

$$\therefore \lambda_1 + \lambda_2 + \lambda_3 = \frac{\alpha_1 + \alpha_2 + \alpha_3 + \alpha_1 \alpha_2 \alpha_3 \mu_0 \beta_0 A}{\alpha_1 \alpha_2 \alpha_3 \mu_0 \beta_0 A} \quad (20a)$$

$$\lambda_1 \lambda_2 + \lambda_2 \lambda_3 + \lambda_3 \lambda_1 = \frac{\alpha_1 \alpha_2 + \alpha_2 \alpha_3 + \alpha_3 \alpha_1 + \alpha_1 \alpha_2 \alpha_3 \mu_0 \beta_0 B}{\alpha_1 \alpha_2 \alpha_3 \mu_0 \beta_0 A} \quad (20b)$$

$$\lambda_1 \lambda_2 \lambda_3 = \frac{\alpha_1 \alpha_2 \alpha_3 (I + \mu_0 \beta_0)}{\alpha_1 \alpha_2 \alpha_3 \mu_0 \beta_0 A} \quad (20c)$$

The type of indicial response obtained depends on the nature of λ_1, λ_2 and λ_3 : they are either all real, or two of them are conjugate complex numbers. If two of the factors are complex, the response will be oscillatory, so we need only consider the cases in which the factors are real. If λ_1, λ_2 and λ_3 are real and positive, equation (19) is of the same form as that for the gain of an amplifier without feedback having stages with time constants $I/\lambda_1, I/\lambda_2, I/\lambda_3$ [c.f. Equ. (17)]. Since the time constants of the stages and the feedback factor determine the product $\lambda_1 \lambda_2 \lambda_3$ independently of the ratios $\lambda_1 : \lambda_2 : \lambda_3$ (Equ. 20c), it can be shown⁶ that the smallest rise time is obtained for the indicial response when $\lambda_1 = \lambda_2 = \lambda_3$: this is the condition for the feedback amplifier to be critically damped.

5.1. Three-stage amplifier with constant β

If $\beta = \beta_0$ and $\lambda_1 = \lambda_2 = \lambda_3 = \alpha$, then

$$3\alpha = \alpha_1 + \alpha_2 + \alpha_3 \quad (21a)$$

$$3\alpha^2 = \alpha_1 \alpha_2 + \alpha_1 \alpha_3 + \alpha_3 \alpha_1 \quad (21b)$$

$$\alpha^3 = \alpha_1 \alpha_2 \alpha_3 (I + \mu_0 \beta_0) \quad (21c)$$

These equations cannot be satisfied unless $\mu_0 \beta_0 = 0$, or $\alpha_1 = \alpha_2 = \alpha_3 = 0$ or unless $\alpha_1,$

α_2 or α_3 is complex. It is therefore impossible to obtain three equal factors to the denominator of the indicial response of a three-stage resistance-coupled amplifier with a negative-feedback path whose transfer coefficient is independent of frequency. Brockelsby and Mayr found that it was impossible to obtain a maximally-flat frequency response of the form $|A_0/A(\omega)|^2 = 1 + X^6$ (where X is the normalized frequency) for a three-stage amplifier with constant β .

5.2. Three-stage amplifier with a single time constant in the feedback path.

If $\beta(p)I = \beta_0 \frac{p + \alpha_4}{\alpha_4} I$ and $\lambda_1 = \lambda_2 = \lambda_3 = \alpha$,

then

$$3\alpha = \alpha_1 + \alpha_2 + \alpha_3 \quad (22a)$$

$$3\alpha^2 = \alpha_1 \alpha_2 + \alpha_2 \alpha_3 + \alpha_3 \alpha_1 + \frac{\alpha_1 \alpha_2 \alpha_3}{\alpha_4} \mu_0 \beta_0 \quad (22b)$$

$$\alpha^3 = \alpha_1 \alpha_2 \alpha_3 (I + \mu_0 \beta_0) \quad (22c)$$

$$\therefore \alpha = \frac{1}{3}(\alpha_1 + \alpha_2 + \alpha_3) = [\alpha_1 \alpha_2 \alpha_3 (I + \mu_0 \beta_0)]^{1/3} \quad (23)$$

$$\alpha_4 = \frac{3\alpha_1 \alpha_2 \alpha_3 \mu_0 \beta_0}{\alpha_1^2 + \alpha_2^2 + \alpha_3^2 - (\alpha_1 \alpha_2 + \alpha_2 \alpha_3 + \alpha_3 \alpha_1)} \quad (24)$$

$$I + \mu_0 \beta_0 = \frac{(\alpha_1 + \alpha_2 + \alpha_3)^3}{27\alpha_1 \alpha_2 \alpha_3} \quad (25)$$

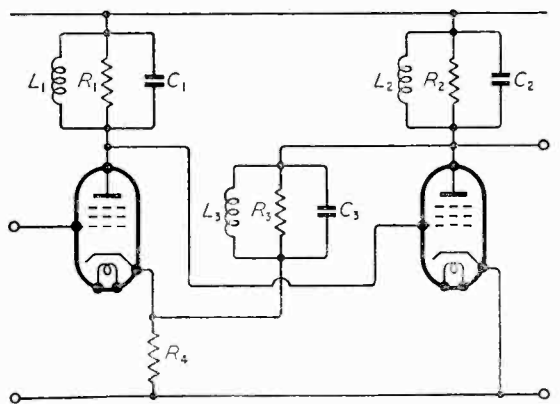


Fig. 12. Band-pass circuit equivalent to the low-pass circuit of Figs. 2 and 5.

It is seen that for any given time constants for the three stages of the amplifier, three equal factors can only be obtained for the particular value of the feedback factor given by Equ. (25).

5.3. Three-stage amplifier with two time constants in the feedback path

$$\text{If } \beta(p)\mathbf{1} = \beta_0 \frac{p + \alpha_4}{\alpha_4} \frac{p + \alpha_5}{\alpha_5} \mathbf{1}$$

and $\lambda_1 = \lambda_2 = \lambda_3 = \alpha$, then

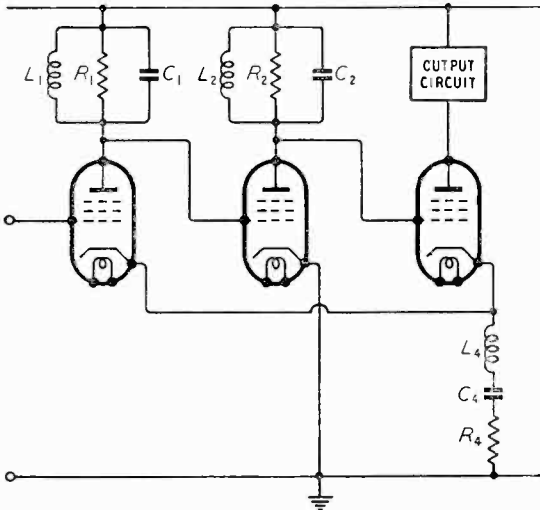


Fig. 13. Band-pass circuit equivalent to the low-pass circuit of Figs. 3 and 6.

$$\alpha^3 = \alpha_1 \alpha_2 \alpha_3 (\mathbf{1} + \mu_0 \beta_0) \quad \dots \quad (26c)$$

$$\therefore \alpha_4, \alpha_5 = \frac{\mathbf{1}}{2a} \left(b \mp \sqrt{b^2 - 4ac} \right) \quad \dots \quad (27)$$

where

$$a = 3\alpha - (\alpha_1 + \alpha_2 + \alpha_3)$$

$$b = 3\alpha^2 - (\alpha_1 \alpha_2 + \alpha_2 \alpha_3 + \alpha_3 \alpha_1)$$

$$c = \alpha^3 - \alpha_1 \alpha_2 \alpha_3$$

Three equal factors can therefore be obtained for any given time constants for the three stages provided that

$$\mathbf{1} + \mu_0 \beta_0 > \frac{(\alpha_1 + \alpha_2 + \alpha_3)^3}{27\alpha_1 \alpha_2 \alpha_3}$$

When

$$\mathbf{1} + \mu_0 \beta_0 = \frac{(\alpha_1 + \alpha_2 + \alpha_3)^3}{27\alpha_1 \alpha_2 \alpha_3},$$

α_4 or α_5 becomes infinite and the circuit reduces to that of Sec. 5.2 having only one time constant in the feedback path.

$$\text{When } \mathbf{1} + \mu_0 \beta_0 < \frac{(\alpha_1 + \alpha_2 + \alpha_3)^3}{27\alpha_1 \alpha_2 \alpha_3},$$

equal factors cannot be obtained and the tran-

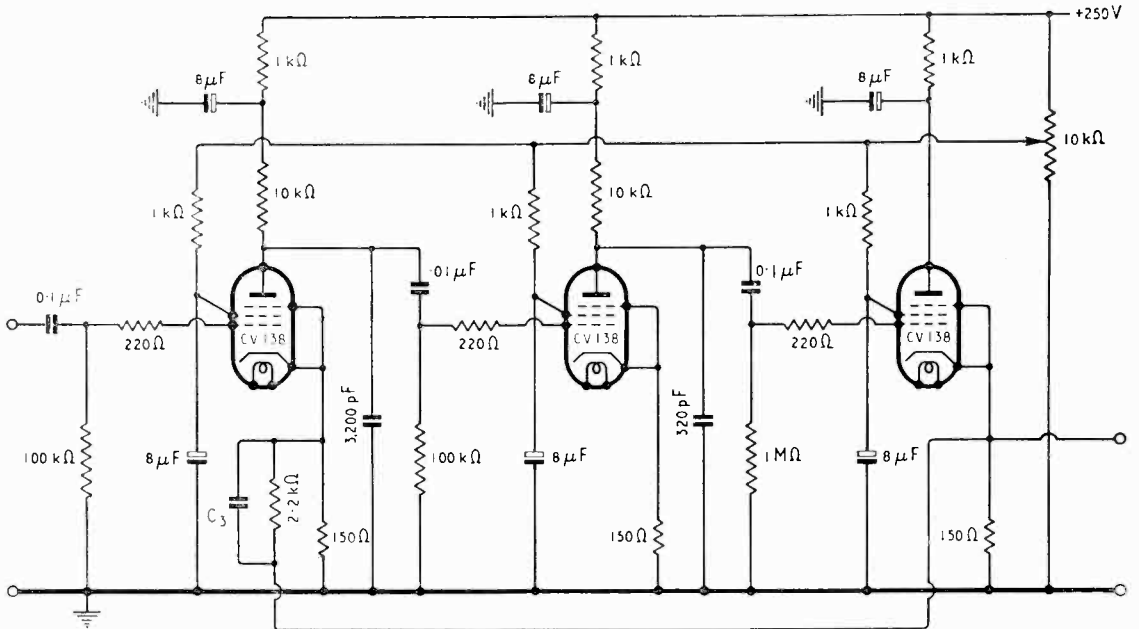


Fig. 14. Circuit of experimental amplifier.

$$3\alpha = \alpha_1 + \alpha_2 + \alpha_3 + \mu_0 \beta_0 \frac{\alpha_1 \alpha_2 \alpha_3}{\alpha_4 \alpha_5} \quad \dots \quad (26a)$$

$$3\alpha^2 = \alpha_1 \alpha_2 + \alpha_2 \alpha_3 + \alpha_3 \alpha_1 + \alpha_1 \alpha_2 \alpha_3 \frac{\alpha_4 + \alpha_5}{\alpha_4 \alpha_5} \mu_0 \beta_0 \quad \dots \quad (26b)$$

sient response is over damped and less rapid.

When equation (27) is satisfied

$$h(p)\mathbf{1} = \frac{\mu_0 \alpha_1 \alpha_2 \alpha_3}{(p + \alpha)^3} \mathbf{1}$$

where

$$x^3 = x_1 x_2 x_3 (1 + \mu_0 \beta_0) \quad \dots \quad (26c)$$

$$\therefore h(p)1 = \frac{\mu_0}{1 + \mu_0 \beta_0} \frac{x^3}{(p + x)^3} 1 \quad \dots \quad (15)$$

and

$$h(t) = \frac{\mu_0}{1 + \mu_0 \beta_0} \left[1 - e^{-x \left(1 + xt + \frac{x^2 t^2}{2} \right)} \right], t > 0 \quad \dots \quad (16)$$

A particularly simple special case is obtained when

$$x_2 = x_3 = x_1 (1 + \mu_0 \beta_0),$$

then $x = x_5 = x_4 = x_3 = x_2 = x_1 (1 + \mu_0 \beta_0)$.

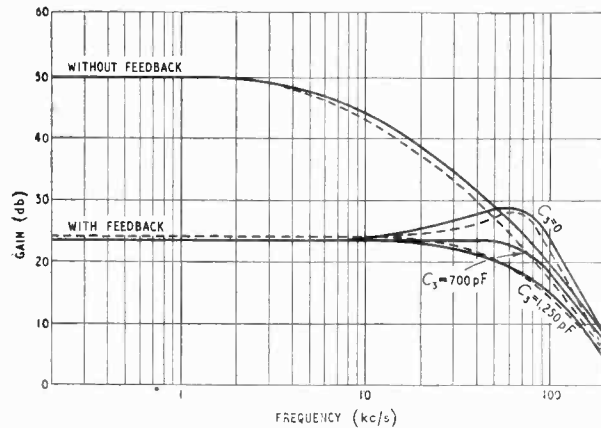


Fig. 15. Measured (solid line) and calculated (dashed line) response curves for the amplifier of Fig. 14.

6. Band-pass Amplifiers

The amplifier circuits so far considered have had low-pass frequency characteristics. A low-pass circuit can be transformed to an equivalent band-pass circuit by replacing each inductance with a series resonant circuit and each capacitance with a parallel resonant circuit⁷.

The envelope of the response of the band-pass circuit to an input voltage of the mid-band frequency, amplitude-modulated by a unit step, is then approximately the indicial response of the equivalent low-pass circuit⁷.

The band-pass equivalent of the circuit of Fig. 2, modified as in Fig. 5, is shown in Fig. 12, each resonant circuit being tuned to the same frequency. The envelope of its response is therefore given by equation (11) if the time constant of the feedback path is given by equation (13). For the band-pass circuit, the time constants of the stages are given by $1/x_1 = 2R_1 C_1$, etc.

The band-pass equivalent of the circuit of Fig. 3, modified as in Fig. 6, is shown in Fig. 13, each resonant circuit being tuned to the same frequency. This circuit has recently been described by Clifford⁸, and is claimed to be remarkable for its simplicity and high performance.

7. Experimental Results

Fig. 14 shows an amplifier which was built in order to obtain experimental verification of the theory. Capacitors were connected between the anode of each stage and earth so that the total interstage capacitances (including valve and wiring capacitances) had the values shown. The time constant of one stage was ten times that of the other. The screen voltage of the valves was adjusted so that the gain at low frequencies with the feedback path disconnected was 50 db, then $\mu_0 \beta_0 = 20$ and Fig. 11 should show the gain-frequency characteristics of the amplifier with and without feedback. The value of capacitance required to be connected across the feedback resistor in order to obtain critical damping [calculated from equation (13)] was 1250 pF.

Fig. 15 shows the measured gain-frequency response of the amplifier without feedback, with an uncompensated feedback path and with capacitance connected across the feedback resistor. Fair agreement is obtained between the measured and calculated values.

Fig. 16 shows oscillograms of the response of the amplifier to a 35- μ s rectangular pulse. The response of the uncompensated amplifier is oscillatory. When the feedback resistor is shunted by a 700-pF capacitor, the response is still oscillatory but the overshoot is less and the oscillation decays more rapidly. When the feedback resistor is shunted by 1250-pF, the response is critically damped. When the feedback resistor is shunted

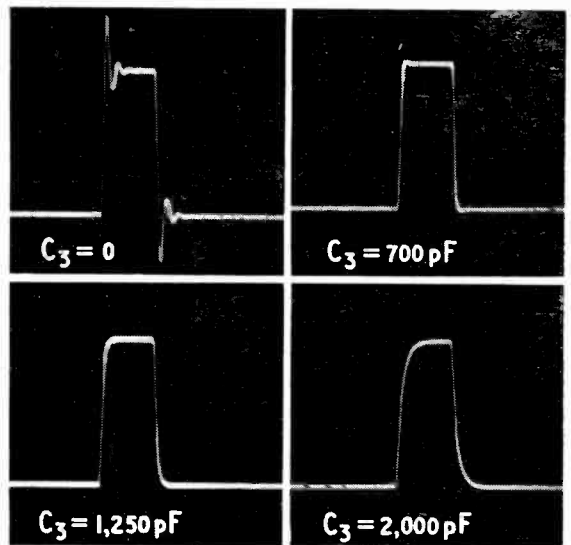


Fig. 16. Response to a 35- μ sec pulse of the amplifier of Fig. 14.

by 2000-pF, the response is over-damped and less rapid.

8. Acknowledgment

Acknowledgment is made to the Engineer-in-Chief of the G.P.O. and to the Controller of H.M. Stationery Office for permission to publish this paper.

REFERENCES

- ¹ C. F. Brockelsby, "Negative Feedback Amplifiers," *Wireless Engineer*, Feb. 1949.
- ² H. Mayr, "Feedback Amplifier Design," *Wireless Engineer*, Sept. 1949.
- ³ V. D. Landon, "Cascade Amplifiers with Maximal Flatness," *R.C.A. Review*, Jan. and April 1941.
- ⁴ H. S. Black, "Stabilized Feedback Amplifiers," *Bell Syst. tech. J.*, Jan. 1934.
- ⁵ H. Bode, "Network Analysis and Feedback Amplifier Design," p. 453. D. Van Nostrand, 1945.
- ⁶ W. C. Elmore, "Transient Response of Damped Linear Networks," *J. Applied Physics*, Jan. 1948.
- ⁷ C. Cherry, "Pulses and Transients in Communication Circuits," Sections 33 and 41. Chapman and Hall, 1949.
- ⁸ British Patent Application No. 13012/49. F. G. Clifford. Improvements in or relating to electron discharge valve amplifiers.

INPUT IMPEDANCE OF TWO CROSSED DIPOLES

By LL. G. Chambers, M.Sc., A.Inst.P.

(Royal Naval Scientific Service)

SUMMARY.—An application of Carter's Method is made to the calculation of the mutual impedance of a pair of crossed dipoles. This is used to give the input impedance of such a crossed pair. It is found that, to a good degree of approximation, the mutual (and input) impedances may be expressed as very simple functions of the angle of separation of the dipoles.

1. Introduction

IN recent years several papers on the calculation of the input impedance of various aerials have appeared. Up to the present, however, calculations on the mutual impedance of a pair of crossed dipoles (see Fig. 1) do not appear to have been made, and it is the purpose of this note to fill this gap in aerial theory. The calculations have been carried through for a pair of infinitely-thin dipoles, each having a total length of half a wavelength. It is thought that the mutual impedance would not be very sensitive to the thickness of the wire forming the dipoles.

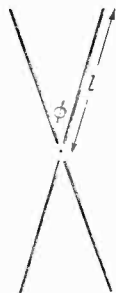


Fig. 1. Pair of crossed dipoles.

2. Field of a Single Dipole

If we have a straight wire, extending along the z axis between $z = a$ and $z = b$, and the charge σ per unit length and the current I both satisfy the wave equation

$$\frac{\partial^2 f}{\partial z_0^2} = \frac{1}{c^2} \frac{\partial^2 f}{\partial t_0^2} \dots \dots \dots \quad (I)$$

(z_0, t_0 being current co-ordinates along the wire), then it has been shown by A. G. D. Watson¹ that

$$4\pi\epsilon E_z = \left[\frac{\sigma(z_0, t - \frac{r'}{c})}{r'} \right]_{z_0=a}^{z_0=b} \dots \dots \quad (2)$$

$$4\pi\epsilon E_\rho = \left[\frac{\sigma(z_0, t - \frac{r'}{c})}{r'} \frac{z_0 - z}{\rho} \right]_{z_0=a}^{z_0=b} \dots \quad (3)$$

where ϵ is the dielectric constant of the medium in which the wire is immersed. The other symbols are explained by Fig. 2.

Simple vector resolution gives us the result that

$$E_r = E_\rho \cos \theta + E_z \sin \theta \dots \dots \quad (4)$$

We now consider the application of this theory to a dipole (Fig. 3). Let us suppose the current distribution in the dipole is given by

$$I = I_0 e^{j\omega t} \frac{\sin k_0(l - |z_0|)}{\sin k_0 l}, \quad (k_0 = \frac{\omega}{c}) \dots \quad (5)$$

Now I and σ are related by

$$\frac{\partial \sigma}{\partial t_0} + \frac{\partial I}{\partial z_0} = 0 \quad (6)$$

$$\frac{\partial \sigma}{\partial z_0} + \frac{1}{c^2} \frac{\partial I}{\partial t_0} = 0 \quad (7)$$

Equation (6) is the equation of continu-

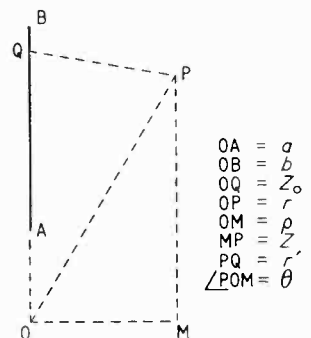


Fig. 2. Co-ordinates for a straight wire; OB is the z-axis.

MS accepted by the Editor, October 1949

ity, and (7) is the condition that I and σ satisfy (1). We note that

$$c = I/\sqrt{\mu\epsilon} \quad \dots \quad (8)$$

and we write

$$R_c = \frac{I}{4\pi\sqrt{\mu\epsilon}} \quad \dots \quad (9)$$

For free space,

$$R_c \approx 30 \text{ ohms} \quad \dots \quad (10)$$

Referring to Fig. 3, it is obvious that

$$r_+^2 = r_+^2 - 2rl \sin \theta + l^2 \quad \dots \quad (11)$$

$$r_-^2 = r_-^2 + 2rl \sin \theta + l^2 \quad \dots \quad (12)$$

At P

$$4\pi\epsilon E_z = \left[\frac{\sigma(l)}{r_+} e^{-jk_0 r_+} - \frac{\{\sigma(+0) - \sigma(-0)\} e^{-jk_0 r}}{r} - \frac{\sigma(-l)}{r_-} e^{-jk_0 r_-} \right] \quad \dots \quad (13)$$

and $4\pi\epsilon E_p =$

$$\left[\frac{\sigma(l)}{r_+} e^{-jk_0 r_+} \cdot \left(\frac{l - r \sin \theta}{r \cos \theta} \right) - \frac{\sigma(-l)}{r_-} e^{-jk_0 r_-} \cdot \left(\frac{-l - r \sin \theta}{r \cos \theta} \right) - \frac{\{\sigma(+0) - \sigma(-0)\} e^{-jk_0 r}}{r} \cdot \left(\frac{-r \sin \theta}{r \cos \theta} \right) \right] \quad (14)$$

where we have now dropped the time factor from (5) and (6).

We deduce

$$\sigma(l) = -\sigma(-l) = \frac{jI_0}{c} \quad \dots \quad (15)$$

$$\sigma(+0) = -\sigma(-0) = -\frac{jI_0}{c} \cos k_0 l \quad \dots \quad (16)$$

The self-impedance Z_s is given by

$$Z_s = -\frac{I}{4\pi\epsilon} \cdot \frac{I}{\sin^2 k_0 l} \int_{-l}^l \frac{j}{c} \left[\frac{e^{-jk_0(l-r)}}{l-r} + \frac{e^{-jk_0(l+r)}}{l+r} + 2 \cos k_0 l \frac{e^{-jk_0 r}}{r} \right] \times \sin k_0 (l - |r|) dr \quad \dots \quad (17)$$

$$= \frac{j R_c}{\sin^2 k_0 l} \int_{-l}^l \left\{ \frac{e^{-jk_0(l-r)}}{l-r} + \frac{e^{-jk_0(l+r)}}{l+r} \right\} \sin k_0 (l - |r|) dr + 2 R_c \frac{\cos k_0 l}{\sin^2 k_0 l} \int_{-l}^l \frac{\sin k_0 r}{r} \sin k_0 (l - |r|) dr \quad \dots \quad (18)$$

If we suppose $k_0 l = \pi/2 + \alpha$, α being integral, Z_s may be shown to reduce to

$$R_c \int_0^{4k_0 l} \frac{1 - e^{-ju}}{u} \alpha u$$

$$= R_c \{(\gamma + \log 4k_0 l - \text{Ci } 4k_0 l) + j \text{Si } 4k_0 l\} \quad (19)$$

which is a well known result (2).

Now if we assume the dipole to be at any resonance the current

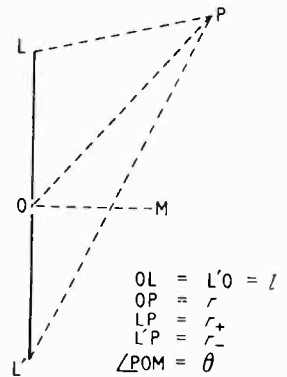
$$= I_0 \frac{\sin k_0 (l - |r|)}{\sin k_0 l} = I_0 \cos k_0 r \quad (20)$$

no matter what resonance is occurring.

The field component E_r is given by

$$E_r = E_p \cos \theta + E_z \sin \theta$$

Fig. 3. Co-ordinates of dipole.



$$= \frac{I}{4\pi\epsilon} \left[\frac{\sigma(l)}{r_+} e^{-jk_0 r_+} \cdot \frac{l}{r} + \frac{\sigma(l)}{r_-} e^{-jk_0 r_-} \cdot \frac{l}{r} \right] \quad (21)$$

3. Calculation of Mutual Impedance

The mutual impedance between two dipoles placed at an angle $\pi/2 - \theta$ to one another is given by integrating the product of the field due to one, tangential to the second, and the current distribution along the second. This process gives us

$$Z_m = -\frac{I}{4\pi\epsilon} \cdot \frac{I}{\sin^2 k_0 l} \cdot \frac{j}{c} \times \int_{-l}^l \left(\frac{e^{-jk_0 r_+}}{r_+} - \frac{e^{-jk_0 r_-}}{r_-} \right) \frac{l}{r} \sin k_0 (l - |r|) dr \quad (22)$$

provided the current distribution in both dipoles is given by (5). If the dipoles are both in resonance we obtain

$$\frac{Z_m}{R_c} = 2j \int_0^l \frac{R}{R} \left\{ \frac{e^{-jR} \pi/2}}{R_+} - \frac{e^{-jR} \pi/2}}{R_-} \right\} \cos \pi/2 R dR = \alpha + j\beta \quad \dots \quad (23)$$

where $r = Rl$, $r_+ = R_+ l$, $r_- = R_- l$. While it is impossible to integrate exactly, these integrals may easily be evaluated by quadrature. The results are given in Table I for the argument $\phi = \pi/2 - \theta$ and plotted in Fig. 4.

It is obvious that

$$Z_m \left(\frac{\pi}{2} + \theta \right) = -Z_m \left(\frac{\pi}{2} - \theta \right) \quad \dots \quad (24)$$

It will be seen that to within 1.5 per cent.

$$\alpha = 1.219 \cos \phi \quad \dots \quad (25)$$

$$\beta = 2.556 - 0.0284\phi \quad \dots \quad (26)$$

Where, in (26), ϕ is measured in degrees.

It may be shown that, for $k_0 l = \pi/2$
 $Z_s = 2R_c\{1.219 + 0.709j\} \dots \dots (27)$

TABLE 1
 $Z_m = 2R_c(\alpha + j\beta)$

ϕ	α	β
0°	1.219	2.561
15°	1.160	2.127
30°	1.054	1.704
45°	0.859	1.269
60°	0.607	0.841
75°	0.314	0.418
90°	0	0

4. Calculation of Input Impedance

If we have a current I divided between two branches of a system, then the equations satisfied are

$$\begin{aligned} V &= I_1 Z_{11} + I_2 Z_{21} \\ &= I_1 Z_{12} + I_2 Z_{22} \dots \dots \dots (28) \end{aligned}$$

The impedance of this two-branch system is given by

$$V = ZI \dots \dots \dots (29)$$

and, if the network is symmetrical,

$$\begin{aligned} Z_{11} &= Z_{22} = Z_s; Z_{21} = Z_{12} = Z_m; \\ I_1 &= I_2 = \frac{1}{2} I \dots \dots \dots (30) \end{aligned}$$

giving

$$2Z = Z_s + Z_m \dots \dots \dots (31)$$

Applying this to our dipole system we have

$$\frac{Z}{R_c} = 1.219(1 + \cos \phi) + j(3.265 - 0.0284\phi^{\circ}) \dots \dots \dots (32)$$

using our approximate relation for Z_m . It will be seen that the radiation resistance vanishes for $\phi = \pi$ (as might have been expected) and that the imaginary part vanishes for $\phi = 115^{\circ}$. It should be noted that these results depend on the current distribution in the dipoles being given by (5).

It is thought that the mutual impedance between two such dipoles should not vary appreciably with their thickness, provided that it is small compared with the length. These results could be applied to a 'fan' of dipoles in a similar manner, provided that the ratio of the maximum currents in each dipole is assumed known.

It will be noticed that the imaginary part of the impedance of a single dipole differs from that of two dipoles separated by a small angle. This is due to the fact that fields may exist

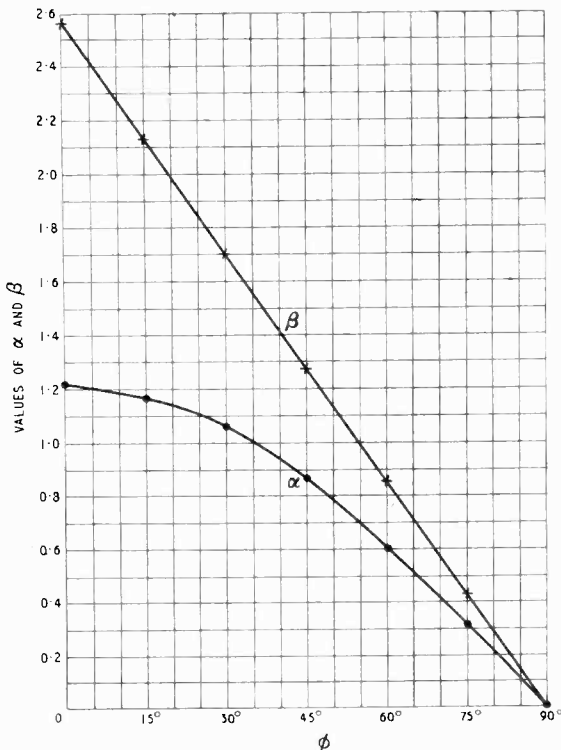


Fig. 4. Plots of the expressions $\alpha = 1.219 \cos \phi$ and $\beta = 2.556 - 0.0284 \phi$.

between the dipoles which, while they affect the reactance, do not affect the resistive part of the impedance which depends only on the field at infinity. This is substantially the same for a single dipole and a pair of dipoles at a very small angle.

5. Acknowledgment

I am indebted to the Admiralty for permission to publish this note.

REFERENCES

- 1 Private Communication.
- 2 P. S. Carter. "Circuit Relations in Radiating Systems" *Proc. Inst. Radio Engrs*, June 1932, Vol. 20, No. 6. Appendix 11.1.

DESIGN OF CATHODE-COUPLED AMPLIFIERS

By S. G. F. Ross, B.E.

(Electrical Engineering Dept., University of Adelaide)

SUMMARY.—This paper contains a brief introductory outline of the advantages and possibilities of cathode-coupled amplifiers. Some recent papers are reviewed, and certain short-comings pointed out. A rigorous theoretical analysis is established, and some experimental results given to show that this analysis can be relied on within the accuracy of published valve data.

1. Introduction

THE use of the normal cathode-follower as a wideband amplifier is well established. Its high input impedance and low output impedance render it capable of good wideband performance, at the same time providing an excellent transformer action where it is necessary to match a high-impedance load into a low-impedance output cable, as in television work.

On the other hand there is a great demand in many fields, such as television, for low noise-level amplifiers. Although triodes are superior in this respect to pentodes, they suffer from lack of sufficient gain, and are subject to adverse Miller effect. The latter difficulty can be overcome by the use of the earthed-grid, or inverted triode. This has found some use in push-pull power-amplifier stages, and is also useful for matching low-impedance input cables into high-impedance receiver circuits, by virtue of its low input impedance.

Several such amplifier stages may be used in cascade in television-receiver circuits. Since the same valve types are applicable to synchronizing and other circuits, this makes for a marked saving in the number of valve types employed, as well as simplifying the coupling circuits required in the video amplifier or r.f. stages employing these valves.

The increasing popularity of this form of amplifier makes it desirable to derive a theoretical analysis which gives a close approximation to experimental results.

Several previous attempts to do this have failed because of the assumption of constant valve parameters. Sziklai and Schroeder¹ made a good start on the problem of the cathode-coupled twin triode. However, careful analysis of the equivalent circuit and valve characteristics shows that their assumption that the valve parameters are equal for each triode section is not justified. For the same reason, Pullen² failed to obtain a set of theoretical curves consistent with those he had obtained experimentally.

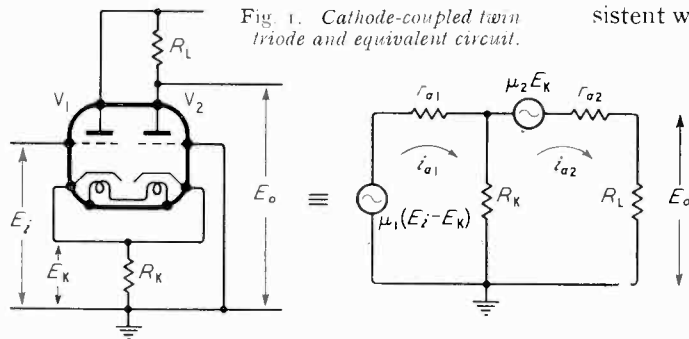


Fig. 1. Cathode-coupled twin triode and equivalent circuit.

2. Graphical Analysis

It is as well to mention here a fairly simple and straightforward graphical analysis evolved by Rifkin.³ This makes use of dynamic valve characteristics which are, however, difficult to determine accurately. The difficulty here arises from the fact that the combined bias voltage lowers the available anode-cathode potential by an equal amount. To take this

The nature of the impedance transformations of the cathode-follower and inverted amplifier opens up the possibility of combining these two amplifiers with a common cathode load. This is what is done in the cathode-coupled (or 'long-tailed') amplifier. Such a combination, using a single twin-triode amplifier, is found to give wideband amplification comparable with that of a pentode, but with very superior signal-to-noise ratio.

into account for any combination of anode load and cathode resistor requires a multiplicity of dynamic curves. Neglect of this effect can introduce substantial errors, especially at low values of anode current, where the values of r_a and μ change rapidly with the current.

3. Theoretical Design Data

The following method of approach, although rather more tedious than that of Rifkin, nevertheless lends itself to easy tabulation and curve

MS accepted by the Editor, November 1949

production. At the same time it is strictly theoretical and consequently is preferable to the more approximate graphical method. Referring to Fig. 1, the formula for the voltage amplification of the cathode-coupled amplifier (as verified in the Appendix) is:

$$A = \frac{E_0}{E_i} = \frac{\mu_1(\mu_2 + 1) R_L R_K}{r_{a1} r_{a2} + r_{a1} R_L + r_{a1} R_K (\mu_2 + 1) + R_K (\mu_1 + 1) (r_{a2} + R_L)}$$

Application of this formula is dependent on the determination of i_{a1} and i_{a2} for any chosen values of R_L and R_K , thereby obtaining r_{a1} , r_{a2} , μ_1 and μ_2 from the valve curves (Fig. 3). The procedure is quite straightforward and is indicated here for a 6SN7 valve using the recommended anode supply of 250 volts.

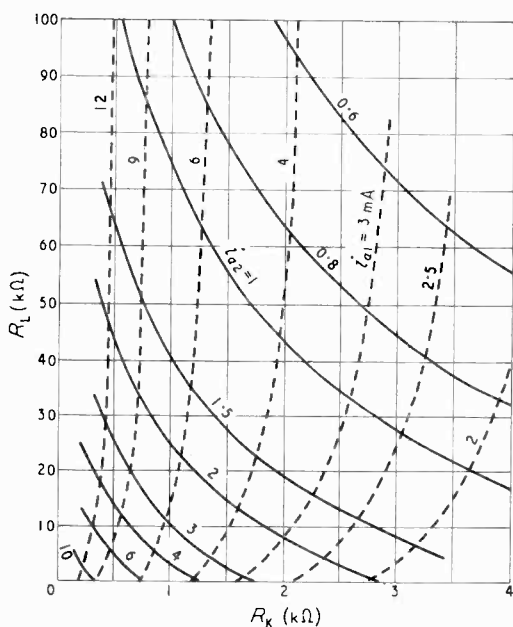


Fig. 2. Anode-current curves for cathode-coupled 6SN7.

Select $i_{a2} = 3\text{mA}$ (constant).

Let bias = -8V .

Then anode-cathode potential of $V_1 = 242\text{V}$.

Whence, from published curves, $i_{a1} = 8\text{mA}$.

$$\therefore R_K = \frac{8}{3 + 8} \times 1,000 = 727\ \Omega.$$

Again, from published curves, anode-cathode potential of $V_2 = 194\text{V}$.

$$\therefore \text{Voltage drop in } R_L = (242 - 194) = 48\text{V}.$$

$$\therefore R_L = \frac{48}{3} \times 1000 = 16,000\ \Omega$$

Table 1 shows in skeleton form how a series of these results can be easily tabulated:

Using this Table, we can draw a set of $R_L - R_K$ curves for constant values of i_{a2} . Since the i_{a1} column is identical for each chosen value of i_{a2} , there will be corresponding i_{a1} points on

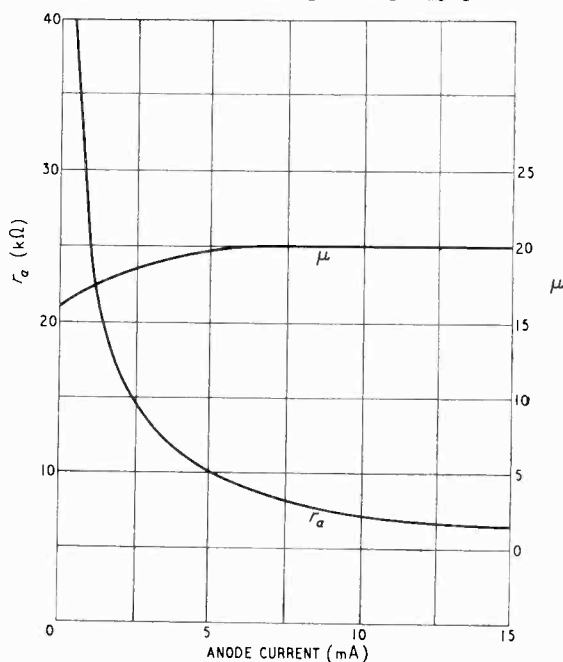


Fig. 3. r_a and μ characteristics of 6SN7.

each curve plotted and, by simple interpolation, a further set of curves may be plotted of constant values of i_{a1} . This process is indicated in Fig. 2, which shows clearly where it is necessary to choose i_{a2} values very closely together in forming the Table.

TABLE 1

BIAS (-V)	i_{a1} (mA)	i_{a2} (mA)	R_L (Ω)	R_K (Ω)	i_{a2}	R_L	R_K	i_{a2}	R_L	R_K	i_{a2}	R_L	R_K
6.0	12.8	0.8	151,800	440	1.0	116,700	435				6.0	9,800	320
6.5	11.6		140,300	520		107,100	520					8,100	370
7.0	10.4		129,400	625		97,500	610					6,300	425
7.25	9.8		124,000	680		92,800	670					5,500	460
11.0	2.1		34,350	3,750		20,800	3,550				—	—	—

When this set of curves has been established it becomes a simple matter to compile a table, such as shown in skeleton form in Table 2, giving r_{a1} , r_{a2} , μ_1 and μ_2 and thence the voltage amplification for any chosen values of R_L and R_K . From this Table we can draw up a final set of curves (the full lines in Fig. 4) from which to choose suitable circuit constants for any required gain.

from normal with high values of anode load. However, the results show that, within the range

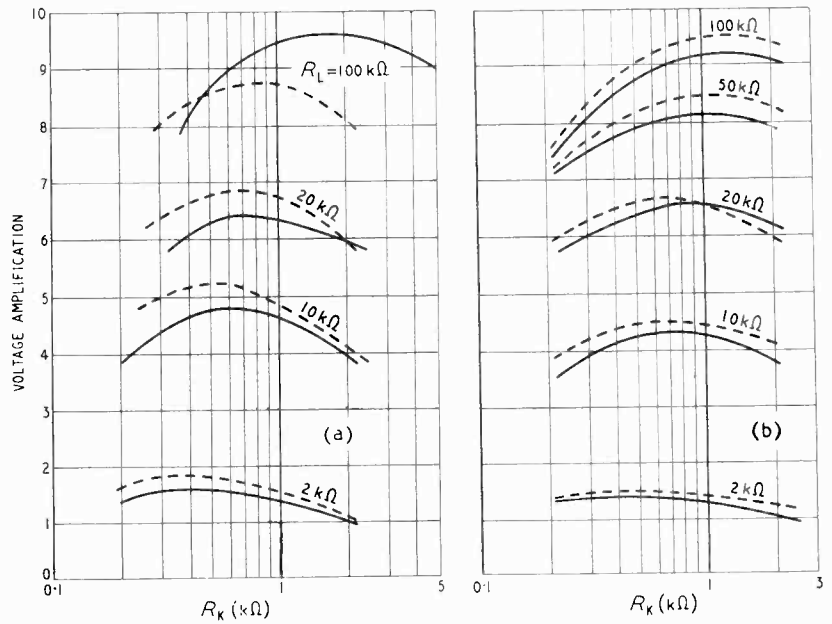


Fig. 4. (a) Comparison of theoretical (full curves) and experimental (broken curves) amplification for cathode-coupled 6SN7; (b) comparison of experimental amplification and theoretical curves (full lines) obtained by plotting individual valve characteristics.

4. Experimental Verification

The curves of Fig. 4 indicate that the theoretical gain is somewhat higher than that obtained experimentally by Pullen. However, he has not stated the anode supply voltage, nor the magnitude of the input signal used. The author has carried out some tests with a single 6SN7, using the same anode supply (regulated 250 volts) as that used in the theoretical treatment, and an input signal of 0.5 volt. The curves obtained are shown by the broken lines in Fig. 4(a). Further tests showed that the amplification dropped off as the magnitude of the input signal was increased, as indicated in Fig. 5. This is due to the unbalanced effect of r_a on the positive and negative half-cycles of current.

The above tests were carried out at a frequency of 100 kc/s, and this accounts for the departure

normally applicable to wideband amplifiers, the agreement between experimental and theoretical results is very good.

5. Precise Test of Accuracy of Theory

The author found that there were appreciable variations of characteristics from valve to valve, in the low cathode-current zones outside the normal operating range. In addition, the static value of r_a is a function, not only of anode current, but also of anode voltage and grid bias. In view of this, and the fairly high frequency employed in the previous test, it was considered that a more exhaustive test of the accuracy of the new formula was desirable.

A sample 6SN7 twin triode was taken, its characteristic curves plotted, and from these the curves of constant i_a derived (as in Fig. 2).

TABLE 2

R_L	R_K	i_{a1}	μ_1	r_{a1}	i_{a2}	μ_2	r_{a2}	A
2,000	200	14.0	20.0	6,500	12.0	20.0	6,700	1.40
	2,000	2.75	18.9	13,300	2.5	18.7	14,000	1.10
10,000	200	15.0	20.0	6,450	7.2	20.0	8,300	3.80
	2,000	3.2	19.2	12,300	1.9	18.3	16,000	4.02
20,000	400	12.0	20.0	6,700	3.65	19.3	11,550	6.13
etc.	2,000	3.5	19.3	11,800	1.5	17.9	18,400	5.94

Having thus obtained values of i_{a1} and i_{a2} for the chosen values of R_L and R_K , the valve parameters for these values were obtained from the characteristic curves for the correct operating points (as regards bias or anode voltage).

These new values were then employed in the formula to obtain the theoretical gain curves. These are plotted in Fig. 4(b) together with experimental curves, obtained by using an input signal of 0.5 volt at a frequency of 1,000 cycles per second.

Allowing for small instrumental errors (these were minimized by the use of the lower frequency) and errors in plotting the characteristics and deriving their slopes, it would seem the agreement of the experimental curves to within 5 per cent of all theoretical gain curves is quite conclusive proof of the first-order accuracy of the formula.

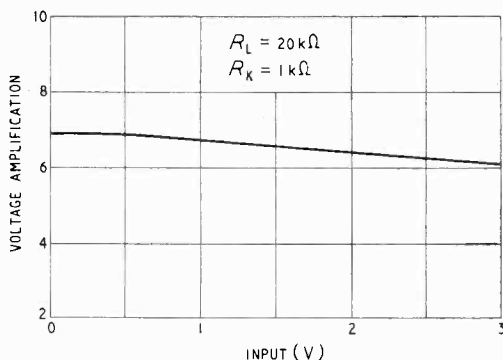


Fig. 5. Amplification as a function of input signal.

6. Conclusions

The foregoing precise analysis leaves us with the assurance that the new formula is accurate. In addition, the curves of Fig. 4 show that the experimental curves can be reasonably duplicated theoretically by applying the formula to published valve data. Consequently, we are free to employ this method, which is as accurate as required for design purposes, and permits interchangeability of valves.

7. Acknowledgment

This work was carried out at the University of Adelaide, under a grant from the Council for Scientific and Industrial Research of Australia, and under the direction of Professor E. O. Willoughby. All assistance given is gratefully acknowledged.

APPENDIX

Verification of the formula used in this paper is a matter of simple algebra.

Considering the equivalent circuit of Fig. 1:—

$$E_K = (i_{a1} - i_{a2}) R_K$$

$$\mu_1(E_i - E_K) - i_{a1} r_{a1} - (i_{a1} - i_{a2}) R_K = 0$$

$$\text{or } \mu_1 R_K (i_{a1} - i_{a2}) + i_{a1} r_{a1} + (i_{a1} - i_{a2}) R_K = \mu_1 E_i$$

$$\therefore i_{a1} [R_K (\mu_1 + 1) + r_{a1}] - i_{a2} R_K (\mu_1 + 1) = \mu_1 E_i$$

$$\text{or } i_{a1} - i_{a2} \cdot \frac{R_K (\mu_1 + 1)}{R_K (\mu_1 + 1) + r_{a1}} = \frac{\mu_1 E_i}{R_K (\mu_1 + 1) + r_{a1}} \quad (1)$$

Again,

$$\mu_2 E_K - i_{a2} (r_{a2} + R_L) - (i_{a2} - i_{a1}) R_K = 0$$

$$\text{or } \mu_2 R_K (i_{a1} - i_{a2}) - i_{a2} (r_{a2} + R_L) - (i_{a2} - i_{a1}) R_K = 0$$

$$\therefore i_{a1} R_K (\mu_2 + 1) - i_{a2} \{ [R_K (\mu_2 + 1) + r_{a2} + R_L] \} = 0$$

$$\text{or } i_{a1} - i_{a2} \cdot \frac{R_K (\mu_2 + 1) + r_{a2} + R_L}{R_K (\mu_2 + 1)} = 0 \quad \dots \quad (2)$$

Subtracting (2) from (1)

$$i_{a2} \left\{ \frac{R_K (\mu_2 + 1) + r_{a2} + R_L}{R_K (\mu_2 + 1)} - \frac{R_K (\mu_1 + 1)}{R_K (\mu_1 + 1) + r_{a1}} \right\} = \frac{\mu_1 E_i}{R_K (\mu_1 + 1) + r_{a1}}$$

$$\therefore i_{a2} = \frac{\mu_1 E_i R_K (\mu_2 + 1)}{r_{a1} r_{a2} + r_{a1} R_L + r_{a1} R_K (\mu_2 + 1) + R_K (\mu_1 + 1) (r_{a2} + R_L)}$$

$$\therefore A = \frac{E_0}{E_i} = \frac{i_{a2} R_L}{E_i}$$

$$= \frac{\mu_1 (\mu_2 + 1) R_L R_K}{r_{a1} r_{a2} + r_{a1} R_L + r_{a1} R_K (\mu_2 + 1) + R_K (\mu_1 + 1) (r_{a2} + R_L)}$$

REFERENCES

- 1 "Cathode-coupled Wide-band Amplifiers," by G. C. Sziklai and A. C. Schroeder, *Proc. Inst. Radio Engrs*, Vol. 33, Oct. 1945, pp. 701-709.
- 2 "The Cathode-coupled Amplifier," by K. A. Pullen, Jr, *Proc. Inst. Radio Engrs*, Vol. 34, pp. 402-407.
- 3 "A Graphical Analysis of the Cathode-Coupled Amplifier," by M. S. Rifkin, *Communications*, Dec. 1946, pp. 16, 42.

INSTITUTE OF PHYSICS

The Summer Meeting of the Industrial Radiology Group will be held at the New Horticultural Hall, Victoria, London, S.W.1., from 25th-28th July 1950. There will also be a Technical Exhibition of the International Congress of Radiology and admission to both will be by ticket, obtainable free from the Institute of Physics, 47, Belgrave Sq., London, S.W.1.

1950 S.I.M.A. EXHIBITION AND SYMPOSIUM

The Electronics section is holding its Annual Exhibition and Symposium at the Examination Hall, Queen Square, London, W.C.1., from Tuesday 5th September to Friday 8th September.

The following papers will be read:

- 5th (afternoon), "Electronic Optics and the Use of Materials," by Professor G. I. Finch.
- 6th (morning), "Recent Improvements in Direct Recording," by W. Bamford.
- 6th (afternoon), "The Vibrating Reed Electrometer and its Application to the Measurement of Small Ionization Currents," by R. Y. Parry and H. W. Finch; "Recent Improvements in pH Measurement," by Electronic Instruments Ltd.
- 7th (morning), "Industrial Batching and Counting," by Cinema Television Ltd.
- 7th (afternoon), "The Measurement of Thickness by Means of Beta Rays," by Baldwin Instrument Co., Ltd.
- 8th (morning), "User Problems in Electronic Instrumentation," by Imperial Chemical Industries Ltd.

Entrance to the Symposium and Exhibition will be by ticket obtainable on application to the Secretary of the Scientific Instrument Manufacturers' Association, 17 Princes Gate, London, S.W.7. Entrance to the exhibition only can be secured on presentation of a trade card.

CORRESPONDENCE

Letters to the Editor on technical subjects are always welcome. In publishing such communications the Editors do not necessarily endorse any technical or general statements which they may contain.

Can H and D be Measured Directly?

SIR,—In the April Editorial you have criticized our methods of measuring H and D , described in *Philips' Research Reports*, April 1949. In this criticism a distinction was made between the directly measurable magnitudes B and E , and the only calculable magnitudes H and D . This distinction is elucidated in *Wireless Engineer*, August 1946, p. 207 as follows: " B and E 'can be determined by measurements at the point'; D and H 'have to be calculated on certain assumptions as to the distribution of . . . electric charge over an area or of the ampere-turns over the magnetic path-length.'" In *Nature*, January 9th, 1937, p. 46, the same idea is formulated in the following way: "It will be seen from the above formulae that E and B are measurable characteristics of the electric and magnetic fields, the former by the force on a stationary charge and the latter by the force on a current or moving charge irrespective of the medium. D and H , however, are not directly measurable concepts . . . D is calculable at any point by dividing a charge . . . by an area; and similarly the magnetizing force is calculable by dividing a current by a length."

In our opinion, only the following statement is correct: It is possible to measure E and B 'directly' with the aid of forces, whereas a 'direct' measuring of D and H cannot be performed by forces. The distinction described in the quoted passages, however, is not real, as we hope to make clear in the following.

The definition of E , on which the usual measurement is based, reads:

$$E = \lim \frac{F}{Q},$$

for the spatial dimensions of Q approaching zero. (F = force; Q = charge).

The definition of B is:

$$B = \lim_{\Delta s \rightarrow 0} \frac{F}{I \Delta s}$$

($I \Delta s$ = element of current).

It is evident that even E and B "are not directly measurable concepts, but calculable by dividing a force by a charge, or by a current element or moving charge." Thus in this respect there is no essential difference between our methods of measuring D and H , and the conventional methods of measuring E and B .

According to your Editorial, the transition to infinitesimally small areas and lengths in the processes of measuring D and H is considered as "a very fictitious experiment." But a similar transition is necessary for measuring E and B : In measuring E the charge Q has to be concentrated at a point; in measuring B the current-element must be infinitesimally short and thin. In this respect there is thus no essential difference between the four methods of measuring either.

Yet a slight distinction might be made. In the concepts of either D or H , the transition to infinitesimally small magnitudes is essential for the concept, whereas in the concepts of E and B this transition may be considered as an important, but not essential, condition. This reasoning can be justified in the following manner. If there were charges and current-elements of infinitesimally small dimensions, it would be possible to measure E exactly by a charge of finite value and also B by a current element of finite value. The values of D and H , on the other hand, can be measured only approximately with discs or solenoids of finite dimensions.

This difference, however, seems to us a very subtle one. Therefore we conclude that in vacuo D and H can be measured as well as E and B . In our paper, we wished only to deny the correctness of the conclusions drawn from the (false) statement that D and H in vacuo are not measurable as separate magnitudes.

As to your remarks concerning the measuring of D and H in matter, we are glad to state that there is no disagreement between you and us. In media without remanence and hysteresis, these methods are good; in a medium with residual magnetism the ideal solenoid must be filled with an unmagnetic insulator, so that we have to do with a cavity experiment, as you already suggested for our D -measuring.

P. CORNELIUS,
H. C. HAMAKER.

Philips' Research Laboratories,
Eindhoven, Holland.

BOOK REVIEW

The Magnetic Amplifier

By J. H. REYNER. Pp. 119, with 72 illustrations and 8 plates. Stuart and Richards, 10 Bramerton Street, London, S.W.3. Price 15s.

The fairly recent development of high-quality transducers has stimulated an ever-increasing interest in transducer techniques and in useful practical applications of magnetic amplifiers. The book under review reflects the rising enthusiasm for the new subject.

The technical structure of a transducer is simple, the device being electrically and mechanically of the stature of an iron-core transformer. The theoretical treatment of its electrical performance requires, however, an unorthodox approach and non-conventional methods of thinking, even if the treatment is based on simplifying assumptions of a sweeping nature.

The object of the book under review is to explain in simple language how a transducer works and a magnetic amplifier functions, and thus to develop a background of general understanding of the broad principles of transducer design. The presentation of the subject-matter is, therefore, essentially descriptive, with numerous illustrations and few mathematical formulæ interspersed in the text.

The author has set himself to stimulate interest and to convey general ideas rather than to be rigorous. Thus any mathematical reasoning is, as far as possible, expressed in familiar terms of elementary a.c. theory.

It would be helpful for the type of reader for whom the book is intended if the presentation of the subject-matter could be slightly re-organized to eliminate one or two unnecessary repetitions of discussion and to avoid one or two irritating interruptions in the development of thought. 'Magnetic field strength' is in some places meant to read 'magnetic flux density,' and 'capacitance' or 'condenser' are sometimes used instead of 'capacitor.'
R. F.

BACK ISSUES

An overseas reader is anxious to obtain a copy of *Experimental Wireless & Wireless Engineer* for March 1930, Vol. 7, or a complete volume for 1930. Any reader who has either available is asked to communicate with the Publishing Dept., Iliffe & Sons, Ltd., Dorset House, Stamford St., London, S.E.1.